# Encapsulation by a Chromium(III)-Containing Bicyclic Ligand Cage. Synthesis, Structures, and Physical Properties of Heterometal Complexes $Cr^{III}MCr^{III}$ [M = $(H^+)_2$, Li(I), Mg(II), Cu(II), Ni(II), Ni(IV), Co(III), Fe(II), Fe(III), Mn(II)]

**Dirk Burdinski,[1a] Frank Birkelbach,[1a] Thomas Weyhermüller,[1a] Ulrich Flörke,[1b] Hans-Jürgen Haupt,[1b] Marek Lengen,[1c] Alfred X. Trautwein,[1c] Eckhard Bill,[1a] Karl Wieghardt,[1a] and Phalguni Chaudhuri*,[1a]**

Max-Planck-Institut für Strahlenchemie, Stiftstrasse 34-36, D-45470 Mülheim an der Ruhr, Germany, Anorganische und Analytische Chemie, Universität-Gesamthochschule Paderborn, D-33098 Paderborn, Germany, and Institut für Physik, Medizinische Universität, D-23538 Lübeck, Germany

*Received August 29, 1997*

Synthesis of linear trinuclear complexes containing the [tris(dimethylglyoximato)-metalate(II)]$^{4-}$ anion as bridging ligand of general formula $[LCr^{III}\{\mu\text{-}(dmg)_3M\}Cr^{III}L]^{1+/2+/3+/4+}$ as perchlorate salts, where M = $(H^+)_2$ (**1** and **2**), absent (**3**), $(H^+)_4$ (**4**), Li(I) (**5**), Mg(II) (**6**), Cu(II) (**7**), Ni(II) (**8**), Ni(IV) (**9**), Co(III) (**10**), Fe(II) (**11**), Fe(III) (**12**) and Mn(II) (**13**), has been achieved by stepwise reactions of the LCr unit with in situ prepared $M(dmg)_3^{n-}$ ions, where L represents 1,4,7-trimethyl-1,4,7-triazacyclononane and $dmg^{2-}$ is the dimethylglyoximato dianion. The clathrochelate complexes **1**−**13** have been characterized on the basis of elemental analysis, mass spectrometry, IR, UV−vis, Mössbauer, and EPR spectroscopies, and variable-temperature (2−295 K) magnetic susceptibility measurements. They are quasi-isostructural with the terminal chromium(III) ions in a distorted octahedral environment, $CrN_3O_3$, and the central metal ions M are six-coordinate, mostly trigonal prismatic, with the $MN_6$ core. The crystal structures of the perchlorate salts of **7**, **8**, and **11** have been determined by single-crystal X-ray crystallography. They crystallize in the monoclinic system, space group *C*2/*c* with the following cell parameters: **7**, $a$ = 29.029(7) Å, $b$ = 12.239(4) Å, $c$ = 14.850(4) Å, $\beta$ = 118.90(2)°, $Z$ = 4; **8**, $a$ = 32.333(6) Å, $b$ = 8.772(2) Å, $c$ = 16.716(3) Å, $\beta$ = 109.51(3)°, $Z$ = 4; **11**, $a$ = 30.941(6) Å, $b$ = 8.777(2) Å, $c$ = 16.801(3) Å, $\beta$ = 96.22(3)°, $Z$ = 4. The structures consist of tris(dimethylglyoximato)-bridged $Cr^{III}M^{II}Cr^{III}$ dications and noncoordinated perchlorate anions, with an intramolecular Cr···Cr distance of ∼7.1 Å. The trinuclear unit Cr−M−Cr is nearly planar exhibiting angles at M in the range 179.0−178.6°, except **7**, with a Cr−Cu−Cr angle of 175.1°. Analysis of the susceptibility data indicates the presence of weak to moderate exchange interactions, both ferro- and antiferromagnetic, between the paramagnetic centers. There are indeed two different coupling constants, $J$ (=$J_{12}$ = $J_{23}$) and $J_{13}$, operative in these clathrochelates. $J_{13}$ represents the exchange interaction between the two terminal Cr(III) centers separated by a large distance of ∼7.1 Å. An analysis of the interacting magnetic orbitals in complexes containing three metal centers is presented. The cyclic voltammograms of the complexes reveal both oxidation and reduction processes and indicate the formation of the uncommon species such as Cu(III), Ni(III), Ni(IV), and low-spin Fe(III). Liquid secondary ion mass spectrometry (L-SIMS) demonstrates the nonfragile character of the complexes examined, together with their nuclearity.

## Introduction

This work stems from our continuing interest in the exchange-coupled heteropolymetallic systems, whose investigations have been proved to be more informative in comparison to those of homopolynuclear complexes. The studies of exchange-coupled polymetallic complexes, in which spin coupling between paramagnetic metals is propagated via a bridging molecule, are relevant to many different scientific areas, ranging from chemistry to solid-state physics and to biology, because of their potential impact in material science, catalysis, and metallobiochemistry. The ubiquitous participation of metal sites involving more than one metal center in metalloproteins has elicited the interest of bioinorganic chemists in such interactions.[2−8]

A few years ago we found a general synthetic route to linear trinuclear complexes containing the [tris(dioximato)metalate(II)]$^{4-}$ anion as bridging ligands.[9] These dioximato-bridged trinuclear complexes of general formula

$$[LM_t^{III/IV}\{\mu\text{-}(dmg)_3M_c^{II}\}M_t^{III/IV}L]^{2+/4+}$$

$$M_t = Fe(III), Mn(III), Mn(IV)$$

$$M_c = Zn(II), Cu(II), Ni(II), Fe(II), Mn(II)$$

have been generated by stepwise reactions of the $LM_t$ unit with in situ prepared $[M_c(dmg)_3]^{4-}$ ions, where L represents the tridentate cyclic amine 1,4,7-trimethyl-1,4,7-triazacyclononane and $dmg^{2-}$ is the dimethylglyoximato dianion.

(1) (a) Max-Planck-Institut für Strahlenchemie. (b) Universität-Gesamthochschule Paderborn. (c) Medizinische Universität Lübeck.
(2) Chaudhuri, P.; Winter, M.; Küppers, H.-J.; Wieghardt, K.; Nuber, B.; Weiss, J. *Inorg. Chem.* **1987**, *26*, 3302.
(3) Chaudhuri, P.; Winter, M.; Della Vedova, B. P. C.; Fleischhauer, P.; Haase, W.; Flörke, U.; Haupt, H.-J. *Inorg. Chem.* **1991**, *30*, 4777.
(4) Chaudhuri, P.; Birkelbach, F.; Winter, M.; Staemmler, V.; Fleischhauer, P.; Haase, W.; Flörke, U.; Haupt, H.-J. *J. Chem. Soc., Dalton Trans.* **1994**, 2313.
(5) Birkelbach, F.; Winter, M.; Flörke, U.; Haupt, H.-J.; Butzlaff, C.; Lengen, M.; Bill, E.; Trautwein, A. X.; Wieghardt, K.; Chaudhuri, P. *Inorg. Chem.* **1994**, *33*, 3990 and references therein.
(6) See for example: (a) Holm, R. H., Solomon, E. I., Guest Editors. *Chem. Rev.* **1996**, *96*, No. 7. (b) Feig, A. L.; Lippard, S. J. *Chem. Rev.* **1994**, *94*, 759. (c) Que, L.; True, A. E. *Prog. Inorg. Chem.* **1990**, *38*, 98. (d) Wieghardt, K. *Angew. Chem.* **1989**, *101*, 1179.

S0020-1669(97)01101-4 CCC: $15.00 © 1998 American Chemical Society
Published on Web 02/14/1998

In this paper, we explore the effects of using Cr(III) as the terminal $M_t$ ions in complexes, which are quasi-isostructural with the $Fe^{III}M^{II}Fe^{III}$, $Mn^{III}M^{II}Mn^{III}$, and $Mn^{IV}M^{II}Mn^{IV}$ centers[3,10] and isoelectronic to the latter. We report the synthesis and magnetic, spectroscopic, and other physical properties of the following compounds:

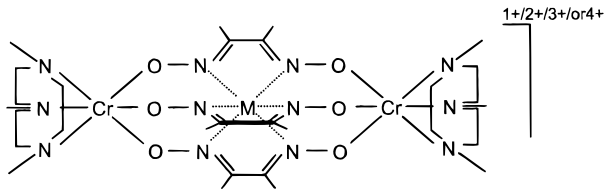


Here M = $(H^+)_2$ (**1** and **2**), absent (**3**), $(H^+)_4$ (**4**), Li(I) (**5**), Mg(II) (**6**), Cu(II) (**7**), Ni(II) (**8**), Ni(IV) (**9**), Co(III) (**10**), Fe(II) (**11**), Fe(III) (**12**), and Mn(II) **13**. These compounds may be considered as coordination complexes containing an ion, $M^{n+}$, totally encapsulated by a metallabicyclic ligand $L^0$, shown as follows:

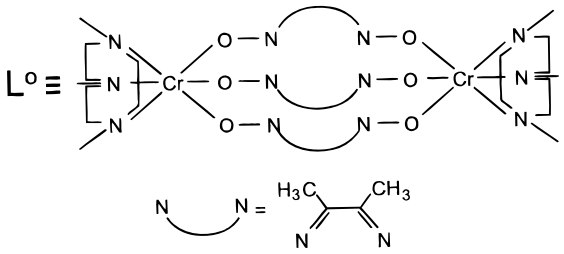


Throughout this paper the compounds **1**−**13** are denoted either by the metal centers only, or as a derivative of $L^0$, for the sake of clarity.

Our trinuclear complexes can be described as clathrochelates,[11] i.e., multicyclic ligand systems that completely encapsulate a metal ion, derived from dioximes and various metal-containing capping agents. A number of clathrochelates of low-spin $d^6$ metal ions, viz. Co(III) and Fe(II), has been readily prepared from various dioximes (e.g. dimethylglyoxime, diphenylglyoxime, cyclohexanedione dioxime) via a template synthesis, where the cobalt or iron serves to orient three dioxime ligands so that they will react with various capping agents such as boron trifluoride, boric acids, $SiCl_4$, and $SnCl_4$ to produce a ligand cage.[12−15] This report, in other words, is concerned with the replacement of boron capping agents by a metal−ligand fragment ML (L is a tridentate amine that coordinates facially in an octahedron) to generate linear trinuclear complexes of type $M_tM_cM_t$, where the subscript "t" stands for the terminal and "c" for the central metal(M) ions. We took the advantage of the relative inertness of the clathrochelate structure and of ML fragment in order to stabilize the otherwise unstable species. A similar strategy has also been used by Drago and Elias[16] to synthesize a series of complexes of the general formula $[Cap(dmg)_3CoCap]^{n+}$, ("Cap" = metal-containing capping agents) including $[(dienCr^{III})(dmg)_3Co^{III}(dienCr^{III})]^{3+}$, where dien represents diethylenetriamine.

## Experimental Section

**Chemicals.** The macrocycle 1,4,7-trimethyl-1,4,7-triazacyclononane ($L = C_9H_{21}N_3$) and its chromium(III) complex $LCrBr_3$ were prepared as described previously.[2,17] All other starting materials were commercially available and mostly of reagent grade. Elemental analyses (C, H, N) were performed by the Microanalytical Laboratory, Ruhr-Universität Bochum. Manganese, iron, and cobalt were determined spectrophotometrically by using pyridine-2,6-dicarboxylic acid;[18] chromium was determined as chromate at $\lambda$ = 370 nm ($\epsilon$ = 4960 $M^{-1}$ $cm^{-1}$). Copper and nickel were determined gravimetrically by using *N*-benzoyl-*N*-phenylhydroxylamine and dimethylglyoxime, respectively. Zinc and lithium were determined by AAS. The perchlorate anion was determined gravimetrically as tetraphenylarsonium perchlorate.

**Physical Measurements.** Fourier transform infrared spectroscopy on KBr pellets was performed on a Perkin-Elmer 1720X FT-IR instrument. Electronic absorption spectra of solutions were measured on a Perkin-Elmer Lambda 9 spectrophotometer.

Magnetic susceptibilities of powdered samples were recorded on a SQUID magnetometer (MPMS, Quantum Design) in the temperature range 2−295 K with an applied field of 1 T. Experimental susceptibility data were corrected for the underlying diamagnetism using Pascal's constants.

The X-band EPR spectra of the polycrystalline material either as solid or in solution were recorded at various temperatures between 3 and 100 K with a Bruker ER 200 D-SRC spectrometer equipped with a standard TE 102 cavity, an Oxford Instruments liquid-helium continuous-flow cryostat, a NMR gaussmeter, a frequency meter, and a data acquisition system.

The Mössbauer spectrometer worked in the conventional constant-acceleration mode with a $^{57}Co/Rh$ source of ca. 1.8 GBq (Amersham Buchler). Isomer shifts are given relative to α-Fe at room temperature.

Cyclic voltammetric experiments were performed with a Princeton Applied Research Model 173 potentiostat−galvanostat driven by a model 175 universal programmer, and details of the experimental procedure have been described earlier.[3]

Positive ion FAB mass spectra were obtained under the condition of liquid secondary ion mass spectrometry (L-SIMS) using $Cs^+$ as the primary ion (22 keV) on a VG Autospectrometer with *m*-nitrobenzyl alcohol as the matrix solvent. The range *m*/*z* = 100−2700 was routinely investigated.

**Preparation of Complexes. $[LCr^{III}\{\mu\text{-}(dmg)_3(H^+)_2\}Cr^{III}L]Br_2\cdot CH_3OH$ (1).** A suspension of green $LCrBr_3$ (0.93 g, 2 mmol),[2] dimethylglyoxime (0.35 g, 3 mmol), and triethylamine (0.8 mL, 6 mmol) in methanol (60 mL) was refluxed for 10 h. The green suspension changed its color to brown in 3−5 h. The reaction is complete when a clear deep red solution is obtained, practically without

(7) (a) *Magnetic Molecular Materials*; Gatteschi, D., Kahn, O., Miller, J. S., Palacio, F., Eds.; NATO ASI Series E, Vol. 198; Kluwer Academic: Dordrecht, The Netherlands, 1990. (b) Kahn, O. *Molecular Magnetisim*; VCH Verlagsgesellschaft: Weinheim, Germany, 1993. (c) Hendrickson, D. N. In *Research Frontiers in Magnetochemistry*; O'Connor, C. J., Ed.; World Scientific: Singapore, 1993; p 87.
(8) (a) Murray, K. S. *Adv. Inorg. Chem.* **1995**, *43*, 261. (b) Kahn, O. *Adv. Inorg. Chem.* **1995**, *43*, 179.
(9) Chaudhuri, P.; Winter, M.; Fleischhauer, P.; Haase, W.; Flörke, U.; Haupt, H.-J. *J. Chem. Soc., Chem. Commun.* **1990**, 1728.
(10) (a) Birkelbach, F.; Flörke, U.; Haupt, H.-J.; Butzlaff, C.; Trautwein, A. X.; Wieghardt, K.; Chaudhuri, P. *Inorg. Chem.*, in press. (b) Birkelbach, F.; Weyhermüller, T.; Lengen, M.; Gerdan, M.; Trautwein, A. X.; Wieghardt, K.; Chaudhuri, P. *J. Chem. Soc., Dalton Trans.* **1997**, 4529.
(11) Busch, D. H. *Rec. Chem. Prog.* **1964**, *25*, 107.
(12) (a) Boston, D. R.; Rose, N. J. *J. Am. Chem. Soc.* **1968**, *90*, 6859. (b) Boston, D. R.; Rose, N. J. *J. Am. Chem. Soc.* **1973**, *95*, 4163. (c) Jackels, S. C.; Rose, N. J. *Inorg. Chem.* **1973**, *12*, 1232.
(13) (a) Parks, J. E.; Wagner, B. E.; Holm, R. H. *J. Am. Chem. Soc.* **1970**, *92*, 3500. (b) Larsen, E.; La Mar, G. N.; Wagner, B. E.; Parks, J. E.; Holm, R. H. *Inorg. Chem.* **1972**, *11*, 2652.
(14) (a) Rai, H. C.; Jena, A. K.; Sahoo, B. *Inorg. Chim. Acta* **1979**, *35*, 29. (b) Voloshin, Y. Z.; Kostromina, N. A.; Nazarenko, A. Y. *Inorg. Chim. Acta* **1990**, *170*, 181. (c) Voloshin, Y. Z.; Belsky, V. K.; Trachevskii, V. V. *Polyhedron* **1992**, *11*, 1939.
(15) (a) Kubow, S. A.; Takeuchi, K. J.; Grzybowski, J. J.; Jircitano, A. J.; Goedken, V. L. *Inorg. Chim. Acta* **1996**, *241*, 21. (b) Robbins, M. K.; Naser, D. W.; Heiland, J. L.; Grzybowski, J. J. *Inorg. Chem.* **1985**, *24*, 3381.
(16) Drago, R. S.; Elias, J. H. *J. Am. Chem. Soc.* **1977**, *99*, 6570.
(17) Wieghardt, K.; Chaudhuri, P.; Nuber, B.; Weiss, J. *Inorg. Chem.* **1982**, *21*, 3086.
(18) Hartkamp, H. *Z. Anal. Chem.* **1964**, *199*, 183.
(19) *International Tables for X-ray Crystallography*; Kynoch: Birmingham, England, 1974; Vol. 4.

any green solid. The hot solution was filtered to remove any green solid $LCrBr_3$. The red mother liquor was diluted with 20 mL of water and kept at room temperature for crystallization. The red crystalline product was collected by filtration and air-dried. Yield: 0.55 g (56%). Anal. Calcd for $[C_{30}H_{62}N_{12}O_6Cr_2Br_2 \cdot CH_3OH]$: C, 37.89; H, 6.77; N, 17.10; Cr, 10.58. Found: C, 37.7; H, 7.3; N, 16.9; Cr, 10.3. IR (KBr, $cm^{-1}$): $\nu$(NH) 3230−3200 m, $\nu$(CN) 1622 m, 1589 w, $\nu$(NO) 1186, 1066 s. UV−vis in $CH_3CN$ [$\lambda_{max}$, nm ($\epsilon$, $M^{-1}$ $cm^{-1}$)]: 268 (51 300), 525 (244). MS (*m*/*z*): 871.0, 789.5, 395.2.

The synthesis of the corresponding perchlorate salt $[LCr\{\mu\text{-}(dmg)_3\text{-}(H^+)_2\}CrL](ClO_4)_2 \cdot CH_3OH$ (**2**) has already been published.[20] MS (*m*/*z*): 889.5, 789.6, 395.2.

**$[LCr\{\mu\text{-}(dmg)_3\}CrL]$ (3).** A 2 mL volume of an aqueous solution (40%) of tetrabutylammonium hydroxide was mixed with 4 mL of acetonitrile, and this mixture was added dropwise to a vigorously stirred solution of **2** (0.51 g, 0.5 mmol) in 10 mL of acetonitrile. Stirring was continued for a few minutes even after completion of the addition. The precipitated microcrystalline red product was filtered out and dried in the air. The substance was recrystallized from 100 mL (1:1) of dichloromethane and acetone. Yield: 0.15 g (∼19%). Anal. Calcd for $C_{30}H_{60}N_{12}O_6Cr_2$: C, 45.68; H, 7.67; N, 21.31; Cr, 13.18. Found: C, 45.5; H, 8.3; N, 21.2; Cr, 13.5. IR (KBr, $cm^{-1}$): $\nu$(NO) 1186 m, $\nu$(CN) 1652 s, 1635 s. UV−vis in $CH_3CN$ [$\lambda_{max}$, nm ($\epsilon$, $M^{-1}$ $cm^{-1}$)]: 267 (34 000), 530 (180). MS (*m*/*z*): 789.3, 395.3.

**$[LCr\{\mu\text{-}(dmg)_3(H^+)_4\}CrL](ClO_4)_4 \cdot 2H_2O$ (4).** A 0.51 g (0.5 mmol) amount of **2** dissolved in 50 mL of acetone was treated under vigorous stirring with 2 mL of concentrated $HClO_4$. The precipitated light red microcrystalline solid was immediately filtered out and washed with a minimum amount of acetone. The solid was dried at 40 °C for a few hours to remove the rest of the acetone. Yield: 0.49 g (80%). Anal. Calcd for $C_{30}H_{64}N_{12}O_{22}Cr_2Cl_4 \cdot 2H_2O$: C, 29.37; H, 5.59; N, 13.70; Cr, 8.48; $ClO_4$, 32.43. Found: C, 29.5; H, 5.8; N, 13.7; Cr, 7.8; $ClO_4$, 32.3. IR (KBr, $cm^{-1}$): $\nu$(NH) 3200 w; $\nu$(NO) 1214, 1178; $\nu$(CN) 1636 m. UV−vis in $CH_3CN$ [$\lambda_{max}$, nm ($\epsilon$, $M^{-1}$ $cm^{-1}$)]: 282 (44 800), 516 (300). MS (*m*/*z*): 989.0, 889.1, 789.2, 395.2.

**$[LCr\{\mu\text{-}(dmg)_3Li^{I}\}CrL](ClO_4)$ (5).** To a solution of **2** (0.51 g, 0.5 mmol) in 30 mL of acetone was added 9 mL of a half-saturated solution of $LiOH \cdot H_2O$ in ethanol under vigorous stirring. Immediate precipitation of a red-brown product occurred. The solid was separated by filtration, washed with a few milliliters of cold acetone, and air-dried. Yield: 0.26 g (57%). Anal. Calcd for $C_{30}H_{60}N_{12}O_6Cr_2Li(ClO_4)$: C, 40.25; H, 6.76; N, 18.77; Cr, 11.62; Li, 0.78; $ClO_4$, 11.11. Found: C, 40.1; H, 7.1; N, 18.8; Cr, 11.5; Li, 0.8; $ClO_4$, 11.0. IR (KBr, $cm^{-1}$): $\nu$(NO) 1154; $\nu$(CN) 1587. UV−vis in $CH_3CN$ [$\lambda_{max}$, nm ($\epsilon$, $M^{-1}$ $cm^{-1}$)]: 263 (53 300), 437 (900), 550 (190). MS (*m*/*z*): 795.2, 398.2.

**$[LCr\{\mu\text{-}(dmg)_3Mg^{II}\}CrL](ClO_4)_2$ (6).** A solution of **2** (0.51 g, 0.5 mmol), hydrated $Mg(ClO_4)_2$ containing ≈83% $Mg(ClO_4)_2$ (2.7 g, 10 mmol), and triethylamine (0.2 mL, 1.4 mmol) in $CH_3CN$ (100 mL) was refluxed for 20 h. The clear red solution was treated with a solution of $NaClO_4 \cdot H_2O$ (3.0 g, 21 mmol) in a few milliliters of acetonitrile and was concentrated to ca. 20 mL to yield a very pale red-brown solid, which was separated by filtration. The solid was treated 2−3 times with a solvent mixture of chloroform (20 mL) and dichloromethane (80 mL), and the suspension was heated to reflux for 0.5 h. The collected filtrate on slow concentration yielded **6** as red-brown needles. It was recrystallized from chloroform/dichloromethane. Yield: 0.20 g (40%). Anal. Calcd for $C_{30}H_{60}N_{12}O_6Cr_2Mg(ClO_4)_2$: C, 35.60; H, 5.98; N, 16.61; Cr, 10.28; Mg, 2.40; $ClO_4$, 19.8. Found: C, 35.2; H, 6.1; N, 16.5; Cr, 10.0; $ClO_4$, 19.3. IR (KBr, $cm^{-1}$): $\nu$(NO) 1184; $\nu$(CN) 1592. UV−vis in $CH_3CN$ [$\lambda_{max}$, nm ($\epsilon$, $M^{-1}$ $cm^{-1}$)]: 209 (28 000), 267 (38 000), 426 (970), 526 (270). MS (*m*/*z*): 911.0, 811.2, 406.2.

**$[LCr\{\mu\text{-}(dmg)_3Cu^{II}\}CrL](ClO_4)_2 \cdot CH_3OH$ (7).** A suspension of $LCrBr_3$ (0.93 g, 2.0 mmol), dimethylglyoxime (0.35 g, 3.0 mmol), $Cu(ClO_4)_2 \cdot 6H_2O$ (0.37 g, 1.0 mmol), and triethylamine (2.0 mL, 14 mmol) in methanol (80 mL) was refluxed for 12−15 h. The reaction was complete when there was no solid present and a clear deep red solution was obtained. The hot solution was eventually filtered to remove any solid particle, and a solution of $NaClO_4 \cdot H_2O$ (2.0 g, 14 mmol) in methanol was added to it. The solution yielded after 2−3 days deep brown crystals of **7** which lost $CH_3OH$ on exposure to air. The substance can be recrystallized from methanol. Yield: 0.75 g (69%). Anal. Calcd for $C_{30}H_{60}N_{12}O_6Cr_2Cu(ClO_4)_2 \cdot CH_3OH$: C, 34.37; H, 5.95; N, 15.51; Cr, 9.60; Cu, 5.87; $ClO_4$, 18.36. Found: C, 33.7; H, 5.85; N, 15.4; Cr, 9.6; Cu, 6.3; $ClO_4$, 18.4. IR (KBr, $cm^{-1}$): $\nu$(NO) 1198 s; $\nu$(CN) 1595 s. UV−vis in $CH_3CN$ [$\lambda_{max}$, nm ($\epsilon$, $M^{-1}$ $cm^{-1}$)]: 273 (48 100), 400 sh (3000), 512 (379), 1019 (73). MS (*m*/*z*): 1074.2, 996.1, 950.3, 851.4, 779.2, 425.9.

**$[LCr\{\mu\text{-}(dmg)_3Ni^{II}\}CrL](ClO_4)_2$ (8).** To a solution of **2** (0.51 g, 0.5 mmol) and triethylamine (0.2 mL, 1.4 mmol) in methanol (50 mL) was added a solid sample of $NiCl_2 \cdot 6H_2O$ (2.38 g, 10 mmol). The red solution was refluxed for 4−5 days, when the solution at the end became dark colored. The solution was filtered hot to remove any brown solid and treated with a solution of $NaClO_4 \cdot H_2O$ (0.8 g, 5.7 mmol) in methanol. Within 0.5 h a precipitation of a deep red microcrystalline substance occurred, which was filtered off and air-dried. X-ray-quality crystals were obtained by recrystallization from methanol/acetone. Yield: 0.32 g (60%). Anal. Calcd for $C_{30}H_{60}N_{12}O_6Cr_2Ni(ClO_4)_2$: C, 34.43; H, 5.78; N, 16.06; Cr, 9.94; Ni, 5.61; $ClO_4$, 19.01. Found: C, 34.2; H, 5.9; N, 16.00; Cr, 9.8; Ni, 5.5; $ClO_4$, 18.5. IR (KBr, $cm^{-1}$): $\nu$(NO) 1189 s; $\nu$(CN) 1591 s. UV−vis in $CH_3CN$ [$\lambda_{max}$, nm ($\epsilon$, $M^{-1}$ $cm^{-1}$)]: 251 (51 500), 439 (838), 538 (318), 880 (47). MS (*m*/*z*): 944.9, 846.1, 423.2.

**$[LCr\{\mu\text{-}(dmg)_3Ni^{IV}\}CrL](ClO_4)_4$ (9).** To an argon-scrubbed acetonitrile (40 mL) solution of **8** (0.21 g, 0.2 mmol) was added one drop of concentrated $HClO_4$ and 0.06 g (0.5 mmol) of $NO(ClO_4)$. The color of the solution changed immediately from deep red to nearly black. After being stirred at ambient temperature for 60 min, it was treated with a solution of dry $NaClO_4$ (0.2 g, 1.6 mmol) in acetonitrile. Slow evaporation of the solvent under argon yielded within 2 days a dark crystalline precipitate, which was filtered off, washed with cold acetonitrile, and air-dried. Yield: 0.17 g (68%). Anal. Calcd for $C_{30}H_{60}N_{12}O_6Cr_2Ni(ClO_4)_4$: C, 28.93; H, 4.86; N, 13.50; Cr, 9.64; Ni, 4.71; $ClO_4$, 31.94. Found: C, 28.7; H, 5.0; N, 13.50, Cr, 9.5; Ni, 4.6; $ClO_4$, 31.6. IR (KBr, $cm^{-1}$): $\nu$(NO) 1209, $\nu$(CN) 1581. UV−vis in $CH_3CN$ [$\lambda_{max}$ ($\epsilon$, $M^{-1}$ $cm^{-1}$)]: 268 (44 500), 455 sh (3100), 503 (3600), 620 sh (1460).

**$[LCr\{\mu\text{-}(dmg)_3Co^{III}\}CrL](ClO_4)_3 \cdot CH_3OH$ (10).** A solution containing **2** (0.51 g, 0.5 mmol) and triethylamine (0.2 mL, 1.4 mmol) in methanol (30 mL) was flushed with argon for ca. 10 min, charged with $Co(ClO_4)_2 \cdot 6H_2O$ (1.83 g, 5 mmol), and heated to reflux for 3 h under the argon atmosphere, whereupon a brown solid precipitated out from the brown solution. The suspension was cooled to ambient temperature in the presence of air to filter off the solid and then air-dried. Long fine red-brown crystalline needles were obtained by recrystallization from methanol/acetone. Yield: 0.35 g (60%). Anal. Calcd for $C_{30}H_{60}N_{12}O_6Cr_2Co(ClO_4)_3 \cdot CH_3OH$: C, 31.60; H, 5.48; N, 14.27; Cr, 8.83; Co, 5.00; $ClO_4$, 25.33. Found: C, 31.2; H, 5.5; N, 14.1; Cr, 8.8; Co, 5.4; $ClO_4$, 25.2. IR (KBr, $cm^{-1}$): $\nu$(NO) 1219, $\nu$(CN) 1588. UV−vis in $CH_3CN$ [$\lambda_{max}$, nm ($\epsilon$, $M^{-1}$ $cm^{-1}$)]: 247 (50 800), 335 sh (7800), 429 sh (1060), 523 sh (420). MS (*m*/*z*): 1045.1, 946.2, 847.3, 473.3, 423.5.

**$[LCr\{\mu\text{-}(dmg)_3Fe^{II}\}CrL](ClO_4)_2 \cdot H_2O$ (11).** Under an argon-blanketing atmosphere, **2** (0.51 g, 0.5 mmol), triethylamine (0.83 mL, 6.0 mmol), and $Fe(ClO_4)_2 \cdot 6H_2O$ (1.81 g, 6.0 mmol) in methanol (40 mL) were heated to reflux for 24 h, during which time a deep red microcrystalline solid precipitated out. The suspension was treated with a solution of $NaClO_4 \cdot H_2O$ (0.80 g, 5.7 mmol) in methanol and cooled to room temperature. The deep red precipitate was filtered off, washed with cold methanol, and recrystallized from methanol/acetone. Deep red X-ray-quality crystals were obtained. Yield: 0.48 g (90%). Anal. Calcd for $C_{30}H_{60}N_{12}O_6Cr_2Fe(ClO_4)_2 \cdot H_2O$: C, 33.94; H, 5.89; N, 15.83; Cr, 9.80; Fe, 5.26; $ClO_4$, 18.73. Found: C, 33.8; H, 5.8; N, 15.6; Cr, 9.6; Fe, 5.0; $ClO_4$, 18.6. IR (KBr, $cm^{-1}$): $\nu$(NO) 1198, $\nu$(CN) 1556. UV−vis in $CH_3CN$ [$\lambda_{max}$, nm ($\epsilon$, $M^{-1}$ $cm^{-1}$)]: 214 (59 000), 296 (18 700), 493 (10 000). MS (*m*/*z*): 1042.0, 943.1, 843.3, 422.2.

**$[LCr\{\mu\text{-}(dmg)_3Fe^{III}\}CrL](ClO_4)_3$ (12).** Nitrosyl perchlorate, $NO(ClO_4)$ (∼150 mg), was added to a solution of **11** (0.41 g, 0.38 mmol) in acetone (300 mL) whereupon the color of the solution changed to

(20) Burdinski, D.; Birkelbach, F.; Gerdan, M.; Trautwein, A. X.; Wieghardt, K.; Chaudhuri, P. *J. Chem. Soc., Chem. Commun.* **1995**, 963.

**Table 1.** Crystallographic Data for $[L_2Cr^{III}_2(dmg)_3Cu^{II}](ClO_4)_2 \cdot CH_3OH$ (**7**), $L_2Cr^{III}_2(dmg)_3Ni^{II}](ClO_4)_2$ (**8**), and $[L_2Cr^{III}_2(dmg)_3Fe^{II}](ClO_4)_2 \cdot H_2O$ (**11**)

| | $Cr_2Cu$ (**7**) | $Cr_2Ni$ (**8**) | $Cr_2Fe$ (**11**) |
|---|---|---|---|
| chem formula | $C_{31}H_{64}N_{12}O_{15}Cl_2Cr_2Cu$ | $C_{30}H_{60}N_{12}O_{14}Cl_2Cr_2Ni$ | $C_{30}H_{62}N_{12}O_{15}Cl_2Cr_2Fe$ |
| fw | 1083.36 | 1046.51 | 1061.66 |
| cryst size, mm | 0.86 × 0.42 × 0.40 | 0.35 × 0.42 × 0.48 | 0.32 × 0.35 × 0.46 |
| cryst system | monoclinic | monoclinic | monoclinic |
| space group | *C*2/*c* | *C*2/*c* | *C*2/*c* |
| *a*, Å | 29.029(7) | 32.333(6) | 30.941(1) |
| *b*, Å | 12.239(4) | 8.772(2) | 8.777(1) |
| *c*, Å | 14.850(4) | 16.716(3) | 16.801(1) |
| $\beta$, deg | 118.90(2) | 109.51(3) | 96.22(3) |
| *V*, Å$^3$ | 4619(2) | 4469(2) | 4536(2) |
| *Z* | 4 | 4 | 4 |
| $\rho_{calc}$, g cm$^{-3}$ | 1.558 | 1.555 | 1.552 |
| diffractometer | Siemens R3 m/V | Siemens SMART | CAD4 |
| $\lambda$ (Mo K$\alpha$), Å | 0.710 73 | 0.710 73 | 0.710 73 |
| $\mu$, mm$^{-1}$ | 1.110 | 1.088 | 0.980 |
| no. of indepdt reflcns ($F > 4.0\sigma(F)$) | 5287 | 4845 | 3294 |
| $R_F$[a] ($F > 4\sigma(F)$) | 6.86 | 3.98 | 4.42 |
| *T*, K | 293(2) | 100(2) | 293(2) |

[a] $R_F = \sum(|F_o| - |F_c|)/\sum|F_o|$.

deep brown and a brown solid appeared. After the mixture was stirred for 10 min at ambient temperature, the microcrystalline brown product was separated by filtration and dried over $P_2O_5$ in a vacuum desiccator. Yield: 0.29 g (67%). Anal. Calcd for $C_{30}H_{60}N_{12}O_6Cr_2Fe(ClO_4)_3$: C, 31.52; H, 5.29; N, 14.70; Cr, 9.67; Fe, 5.19; $ClO_4$, 26.3. Found: C, 31.3; H, 5.2; N, 14.6; Cr, 9.4; Fe, 5.0; $ClO_4$, 26.9. IR (KBr, cm$^{-1}$): $\nu$(NO) 1215, $\nu$(CN) 1574. UV−vis in $CH_3CN$ [$\lambda_{max}$, nm ($\epsilon$, M$^{-1}$ cm$^{-1}$)]: 209 (44 000), 242 (45 000), 485 (3000). MS (*m*/*z*): 1042.1, 943.2, 843.3, 422.3.

**[LCr{$\mu$-(dmg)$_3$Mn$^{II}$}CrL](ClO$_4$)$_2$·CH$_3$OH (13).** To an argon-scrubbed solution of **2** (0.51 g, 0.5 mmol) and triethylamine (0.2 mL, 1.4 mmol) in methanol (80 mL) was added $Mn(ClO_4)_2 \cdot 6H_2O$ (5.13 g, 14 mmol), and the solution was refluxed under argon for 20 h, during which time a brown solid precipitated out. The solid was filtered in the air and recrystallized from methanol/acetone to obtain brown crystals. Yield: 0.27 g (54%). Anal. Calcd for $C_{30}H_{60}N_{12}O_6Cr_2Mn(ClO_4)_2 \cdot CH_3OH$: C, 34.64; H, 6.00; N, 15.64; Cr, 9.68; Mn, 5.11; $ClO_4$, 18.51. Found: C, 34.7; H, 6.0; N, 15.6; Cr, 9.9; Mn, 5.0; $ClO_4$, 18.2. IR (KBr, cm$^{-1}$): $\nu$(NO) 1184, $\nu$(CN) 1583. UV−vis in $CH_3CN$ [$\lambda_{max}$, nm ($\epsilon$, M$^{-1}$ cm$^{-1}$)]: 208 (34 400), 269 (37 200), 420 sh (1140), 526 sh (350), 682 sh (30). MS (*m*/*z*): 942.1, 843.2, 421.5.

*Caution: Perchlorate salts must be handled with care!*

**X-ray Crystal Structure Determinations.** The crystallographic data of $Cr^{III}Cu^{II}Cr^{III}$ (**7**), $Cr^{III}Ni^{II}Cr^{III}$ (**8**), and $Cr^{III}Fe^{II}Cr^{III}$ (**11**) are summarized in Table 1. Graphite monochromated Mo K$\alpha$ X-radiation was used throughout. Intensity data collected at 293 K for **7**, 100 K for **8**, and 293 K for **11** were corrected for Lorentz, polarization, and absorption effects ($\psi$ scans) in the usual manner. The structures were solved by direct methods by using the Siemens SHELXTL-PLUS package (G. M. Sheldrick, Universität Göttingen). The function minimized during full-matrix least-squares refinement was $\sum w(|F_o| - |F_c|)$.[2] Neutral atom scattering factors and anomalous dispersion corrections for non-hydrogen atoms were taken from ref 19. The hydrogen atoms were placed at calculated positions with isotropic thermal parameters; the methyl groups were treated as rigid bodies. All non-hydrogen atoms were refined with anisotropic thermal parameters.

## Results and Discussion

**Preparation of Complexes.** A straightforward, clean, and relatively high-yield synthetic route to pure heterotrinuclear complexes containing the tris($\mu$-dimethylglyoximato) bridge has been developed, as outlined in Scheme 1. The inertness of trivalent chromium ion resulting from a d$^3$ electron configuration and its high thermodynamic stability with the macrocyclic 1,4,7-trimethyl-1,4,7-triazacyclononane are utilized to synthesize Cr(III)−M−Cr(III) trinuclear complexes.

**Scheme 1**

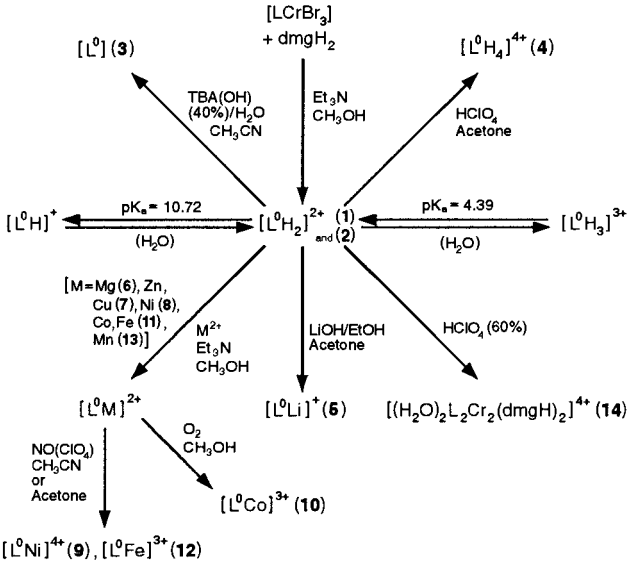


The preparation and crystal structure of the red dimetallic species $[L^0H_2](ClO_4)_2$ (**2**) has been recently described[20] by us, and a schematic view of the 14-membered metallamacrobicycle $L^0$ containing two chromium(III) ions as part of the ring skeleton is shown in the "Introduction".

Complex **1** is just the bromide salt of **2**. Formation of complex **1** and **2** by simple refluxing the $LCr^{3+}$ unit with dimethylglyoxime is an example of spontaneous self-assembly, presumably based on the preference of Cr(III) ions for oxygen donor atoms to azomethine nitrogens.[21] The stable cyclic derivative, present as cation in **1** and **2**, has been proved to be an important precursor for generating various heterometallic trinuclear complexes containing chromium(III) as the terminal ions (i.e. "capping" metals), by replacing the incorporated protons with different metal ions in the presence of a base, viz. $[L_2Cr_2(dmg)_3M]^{1+/2+/3+/4+}$ (M = Li(I), Mg(II), Zn(II), Cu(II), Ni(II), Ni(IV), Co(III), Fe(II), Fe(III) or Mn(II)).

By slow addition of a concentrated aqueous solution of a strong base like tetrabutylammonium hydroxide to the doubly protonated complex **2**, the completely deprotonated form of the macrobicycle, **3**, $L^0$, a neutral species, could be isolated as a red microcrystalline solid. Contrary to **2**, infrared bands of $\nu$-

(21) Burdinski, D. Diploma Thesis, Bochum, 1995.

(NH) are not observed for **3**, indicating the complete deprotonation of the oxime nitrogens in the macrobicycle. As is expected, addition of concentrated $HClO_4$ to a solution of **2** yielded complex **4** containing tetraprotonated oxime nitrogens. In contrast to **2**, stability of the tris(dimethylglyoximato)bridge at a very high concentration of protons in **4** is reduced, as is evidenced by the isolation of a macro*mono*cycle, **14**, from an aqueous perchloric acid solution of **2** (Scheme 1).

The single monocationic complex, $[L^0Li](ClO_4)$, **5**, where $L^0$ is the neutral macrobicycle (i.e. complex **3**), was obtained by neutralizing the protons in **2**, $[L^0H_2](ClO_4)_2$, with a half-saturated solution of LiOH in ethanol. In the absence of a large excess of LiOH, **5** is unstable in protic solvents and **2** is re-formed. Aqueous solution of **5** is strongly basic, as expected. A similar labile behavior of a recently described lithium complex of the sacrophage-type of ligands has been observed.[22]

From a solution of the diprotonated macrobicycle **2** and $Mg(ClO_4)_2$ in acetonitrile to which $NEt_3$ was added, a microcrystalline red-brown precipitate of $[L^0Mg](ClO_4)_2$ (**6**) is obtained (Scheme 1). The ionic radius of $Mg^{2+}$ (86 pm) is very similar to those of $Cu^{2+}$ (87 pm) and $Zn^{2+}$ (88 pm). So it is not very surprising that the $Mg^{2+}$-complex of the macrobicycle is formed.

In general, two different strategies were followed for synthesizing trinuclear complexes. The copper(II) complex **7** was directly prepared by refluxing a suspension of $LCrBr_3$ and dimethylglyoxime with the right stoichiometry in the presence of triethylamine to which metal(II) perchlorate was added. It is conceivable that the central divalent metal ion acts as a template center for the formation of the bicycle. The concept of a template synthesis as a mechanism for the macrobicycle formation has been proposed for the similar B(III)-capped clathrochelates.[12,15] The other strategy involves the substitution of protons from the preformed macrobicycle by the metal centers, like Li, Mg, Ni, Co, Fe, and Mn, that cannot apparently act as centers for the template synthesis.

The trinuclear complex $Cr^{III}Fe^{II}(ls)Cr^{III}$ (**11**), is amenable to oxidation and gives rise to $Cr^{III}Fe^{III}(ls)Cr^{III}$ species, **12**, when oxidized in acetone with $NO^+$. That **12** may be accessible was indicated first by CV experiments. Complex **12** is very susceptible to reduction in solution and decomposes slowly to the reduced form **11**.

Although the complexes $Cr^{III}Ni^{II}Cr^{III}$ (**8**) and $Cr^{III}Ni^{IV}Cr^{III}$ (**9**) could be synthesized in reasonably good yield, all attempts to isolate the species $Cr^{III}Ni^{III}Cr^{III}$ were in vain, presumably because of the small potential difference prevailing between the two higher oxidation states of nickel. That this is indeed the case is demonstrated by isolation of a mixture of **8** and **9** in 1:1 ratio for all attempts to prepare $Cr^{III}Ni^{III}Cr^{III}$ species, which can be ascribed to the following disproportionation reaction

$$2[L^0Ni]^{3+} \rightarrow [L^0Ni]^{2+} + [L^0Ni]^{4+}$$

Complex **9** as a black microcrystalline solid is formed by oxidation of **8** in acetonitrile with $NO(ClO_4)$ in the presence of a small amount of perchloric acid.

**Infrared Spectra.** Since the IR spectra of all complexes are quite similar, the discussion is confined to the most important vibrations of the 4000−400 $cm^{-1}$ region in relation to the structure. Excluding **1** and **3**, all complexes exhibit strong bands near 1090−1100 (antisymmetric stretch) and sharp bands at 620−625 $cm^{-1}$ (antisymmetric band), indicative of uncoordinated perchlorate anions.

The $\nu$(CN) vibration is assigned to the medium strong bands in the wavenumber region 1556−1599 $cm^{-1}$. It is conspicuous that the $\nu$(CN) vibrations of complexes **1**−**4**, without any central metal ion, are situated at a significantly higher frequency, 1622−1652 $cm^{-1}$, than those for other complexes **5**−**13**; for example, there are two intense bands in **3** at 1652 and 1635 $cm^{-1}$. This is in accord with the concept that on complex formation the positively charged $(C_9H_{21}N_3)Cr^{3+}$ unit stabilizes the negative charge on oxygen of the oximate function and thus increases the double bond character of the CN bond, which is expressed as a rise in the frequency of all complexes investigated.[23] Complex **11**, $Cr^{III}Fe^{II}Cr^{III}$, shows the lowest frequency, 1556 $cm^{-1}$, for the $\nu$(CN) vibration, denoting that, in the chelate ring of this complex, more electron delocalization has taken place.

The medium strong to weak bands at 1184−1215 $cm^{-1}$ in the complexes are assignable to the NO stretching vibration.[23] The second NO IR absorption[23a] could not be observed in these complexes, because of the superposition with the bands originating from the perchlorate anions. However, for the bromide salt of the cation in **1** and for the neutral species $L^0$ (**3**), the second NO stretch was identified unambiguously at 1067 and 1068 $cm^{-1}$, respectively.

**Electronic Spectra.** The optical spectra for complexes **1**−**13** have been measured in the range 200−1400 nm in dry acetonitrile to avoid any hydrolysis. The absorption maximum of the free oxime $dmgH_2$ at 224 nm is due to $\pi-\pi^*$ transition of the C═N group and shifts in basic medium due to deprotonation of the OH groups to 218 and 265 nm. Similar $\pi-\pi^*$ transitions of the C═N groups are observed in **1**−**4**, as is evidenced by the bands in the range 267−282 nm with high extinction coefficients ($3.4 \times 10^4-5.1 \times 10^4$ $M^{-1}$ $cm^{-1}$). The bands at 525 nm (244 $M^{-1}$ $cm^{-1}$) for **1** and **2**, ∼530 nm (∼180 $M^{-1}$ $cm^{-1}$) for **3**, and 516 nm (300 $M^{-1}$ $cm^{-1}$) for **4** are assigned to the first spin-allowed transition $^4A_{2g} \rightarrow {}^4T_{2g}$ of the $d^3$ Cr(III) center, noting that the band assignments have been performed by assuming an octahedral ligand field, as the d−d transition of the formula *cis*-$MX_3Y_3$ is not split in the trigonal ($C_{3v}$) ligand field and its energy is equal to $10Dq_{av}$ ($=5Dq_X + 5Dq_Y$),[24] where $Dq_X$ and $Dq_Y$ represent the contributions from the ligands X and Y, respectively. It allows us to approximate the splitting parameter $10Dq$ to lie between 18 900 and 19 400 $cm^{-1}$ for these dichromium(III) complexes **1**−**4** with two $CrN_3O_3$ chromophores.[2,17,25]

All trinuclear complexes with the exception of Fe(II)-/Fe(III)-containing complexes, **11** and **12**, exhibit the lowest-energy spin-allowed transition at the Cr(III) center, similar to only Cr(III)-containing complexes **1**−**4**. Interestingly, **5**−**8** show an additional band in the wavelength range 420−450 nm with extinction coefficients lying between 700 and 1000 $M^{-1}$ $cm^{-1}$. This second band can be ascribed to the $^4A_{2g} \rightarrow {}^4T_{1g}(F)$ transition at the Cr(III) center. This band is missing for all $d^6$ systems, complexes **9**−**11**. The band cannot owe its origin to the metal-to-ligand charge transfer (MLCT) transition, as both the lithium, **5**, and magnesium complex, **6**, without any d-electrons, exhibit also this band. The extinction coefficient of this band is large in comparison to those for the distorted

(22) Anderson, P. A.; Creaser, I. I.; Dean, C.; Harrowfield, J. M.; Horn, E.; Martin, L. L.; Sargeson, A. M.; Snow, M. R.; Tiekink, E. R. T. *Aust. J. Chem.* **1993**, *46*, 449.

(23) (a) Blinc, R.; Hadzi, D. *J. Chem. Soc. A* **1958**, 4536. (b) Burger, K.; Ruff, I.; Ruff, F. *J. Inorg. Nucl. Chem.* **1965**, *27*, 179. (c) Caton, J. E.; Banks, C. V. *Inorg. Chem.* **1967**, *6*, 1670. (d) Chakravorty, A. *Coord. Chem. Rev.* **1974**, *13*, 1.

(24) Krishnamurthy, R.; Schapp, W. B. *J. Chem. Educ.* **1969**, *46*, 799.

(25) Caldwell, S. H.; House, D. A. *J. Inorg. Nucl. Chem.* **1969**, *31*, 811.

**Table 2.** Liquid Secondary Ion Mass Spectra (L-SIMS) Data for Complexes **1**−**13** in the Matrix *m*-Nitrobenzyl Alcohol[a]

| complex | obsd mass (*m*/*z*), assigned ion (relative abundance, %) |
|---|---|
| **1**, $[L^0(H^+)_2]Br_2$ | 871.0, $[L^0(H^+)_2Br]^+$ (1); 789.5, $[L^0(H^+)]^+$ (100); 618.3, $[L^0(H^+) - L]^+$ (4); 395.2, $[L^0(H^+)_2]^{2+}$ (6) |
| **2**, $[L^0(H^+)_2](ClO_4)_2$ | 1011.4, $[L^0(H^+)_2(ClO_4)C_6H_4NO_2]^+$ (2); 989.0, $[L^0(H^+)_2(ClO_4)_2(H)]^+$ (1); 889.5, $[L^0(H^+)_2(ClO_4)]^+$ (60); 789.6 $[L^0(H^+)]^+$ (66); 618.3, $[L^0(H^+) - L]^+$ (7); 395.2, $[L^0(H^+)_2]^{2+}$ (38) |
| **3**, $[L^0]$ | 789.3, $[L^0(H^+)]^+$ (80); 618.3, $[L^0(H^+) - L]^+$ (5); 395.3, $[L^0(H^+)_2]^{2+}$ (35) |
| **4**, $[L^0(H^+)_4](ClO_4)_4$ | 989.0, $[L^0(H^+)_3(ClO_4)_2]^+$ (2); 889.1, $[L^0(H^+)_2(ClO_4)]^+$ (27); 789.2, $[L^0(H^+)]^+$ (7); 618.0, $[L^0(H^+) - L](3)$; 395.2, $[L^0(H^+)_2]^{2+}$ (6) |
| **5**, $[L^0(Li)](ClO_4)$ | 795.2, $[L^0(Li)]^+$ (100); 398.2, $[L^0(H)(Li)]^{2+}$ (7) |
| **6**, $[L^0(Mg)](ClO_4)_2$ | 911.0, $[L^0(Mg)(ClO_4)]^+$ (25); 811.2, $[L^0(Mg) - H]^+$ (10); 406.2, $[L^0(Mg)]^{2+}$ (35) |
| **7**, $[L^0(Cu)]ClO_4)_2$ | 1074.2, $[L^0(Cu)(ClO_4)C_6H_4NO_2]^+$ (3); 996.1, $[L^0(Cu)(ClO_4) + NO_2]^+$ (4); 950.3, $[L^0(Cu)(ClO_4)](100)$; 851.4, $[L^0Cu]^+$ (30); 779.2, $[L^0(Cu)(ClO_4) - L]^+$ (3); 425.9, $[L^0(Cu)]^{2+}$ (28) |
| **8**, $[L^0(Ni)](ClO_4)_2$ | 944.9, $[L^0(Ni)(ClO_4)]^+$ (6); 846.1, $[L^0(Ni)]^+$ (3.5); 675.0, $[L^0(Ni) - L]^+$ (1); 423.2, $[L^0Ni]^{2+}$ (16) |
| **10**, $[L^0(Co)](ClO_4)_3$ | 1045.1, $[L^0(Co)(ClO_4)_2]^+$ (5); 946.2, $[L^0(Co)(ClO_4)]^+$ (17); 847.3, $[L^0(Co)]^+$ (3); 473.3, $[L^0(Co)(ClO_4)]^{2+}$ (5); 423.5, $[L^0(Co)]^{2+}$ (10) |
| **11**, $[L^0(Fe)](ClO_4)_2$ | 1042.0, $[L^0(Fe)(ClO_4)_2]^+$ (2); 943.1, $[L^0(Fe)(ClO_4)]^+$ (50); 843.3, $[L^0(Fe) - H]^+$ (10); 762.2, $[L^0(Fe) - C_4H_6N_2]^+$ (5); 422.2, $[L^0(Fe)]^{2+}$ (40) |
| **12**, $[L^0(Fe)](ClO_4)_3$ | 1042.1, $[L^0(Fe)(ClO_4)_2]^+$ (2); 943.2, $[L^0(Fe)(ClO_4)]^+$ (20); 843.3, $[L^0(Fe) - H]^+$ (2); 422.3, $[L^0(Fe)]^{2+}$ (18) |
| **13**, $[L^0(Mn)](ClO_4)_2$ | 942.1, $[L^0(Mn)(ClO_4)]^+$ (3.5); 843.2, $[L^0(Mn)]^+$ (2); 421.5, $[L^0(Mn)]^{2+}$ (10) |

[a] $L^0$ refers to $C_{30}H_{60}N_{12}O_6Cr_2$ and L to $C_9H_{21}N_3$.

octahedral Cr(III) complexes, probably because of the intensity gain through exchange coupling and of the strong trigonal distortion of the Cr(III) geometry, resulting in a lowering of symmetry to $C_{3v}$.[26,27]

Judged on the basis of extinction coefficients, the bands at 1019 nm for **7** ($Cu^{II}$), 880 nm for **8** ($Ni^{II}$), and 682 nm for **13** ($Mn^{II}$) are ascribed to the d−d transitions at the central M(II) center.

On the basis of high extinction coefficients and similar M → $\pi^*$(oxime) transitions reported in the literature, the peak at 493 nm for **11** ($Fe^{II}$) is thought to be MLCT in character.[28] Complex **9** ($Ni^{IV}$) and **12** ($Fe^{III}$) exhibit respectively a strong band at 455 and 485 nm; these bands owe their origin to the high charge of the respective metal ions and are of L → M charge transfer in nature. The assignment is in complete accord with the earlier observations[29] in Ni(IV) and ls Fe(III) chemistry.

The electronic spectral results indicate that the complexes **1**−**13** are stable and retain their discrete trinuclear entities also in solution.

**Fast Atom Bombardment Mass Spectrometry (FAB-MS).** Mass spectrometry[30] in the L-SIMS mode has been proved to be a very useful analytical tool for characterization of the complexes with the macrobicycle $L^0$ containing Cr(III) ions as a member of the macrobicyclic ring skeleton. A listing of all major signals, excluding the peaks from the matrix, in the fast atom bombardment mass spectra for complexes **1**−**13**, including the assignments, is given in Table 2. The mass spectral results obtained for **2** are described first, because it gives readily interpretable positive ion FAB mass spectrum and the first indication of the diprotonated macrobicycle, $[L^0(H^+)_2]^{2+}$, was obtained from MS before the complete crystal structure of **2** was determined. Shown in Figure 1 is the positive ion FAB mass spectrum of **2**, $[L^0(H^+)_2](ClO_4)_2$, together with the calculated isotope pattern for the important peaks. The two intense peaks centered around *m*/*z* 889 and 395 correspond to ions that have lost one and two perchlorate anions, respectively, from **2**. A species that has lost one proton in addition to two perchlorate anions is observed at *m*/*z* 789 with a relative abundance of 66%. This is an evidence of the robustness of

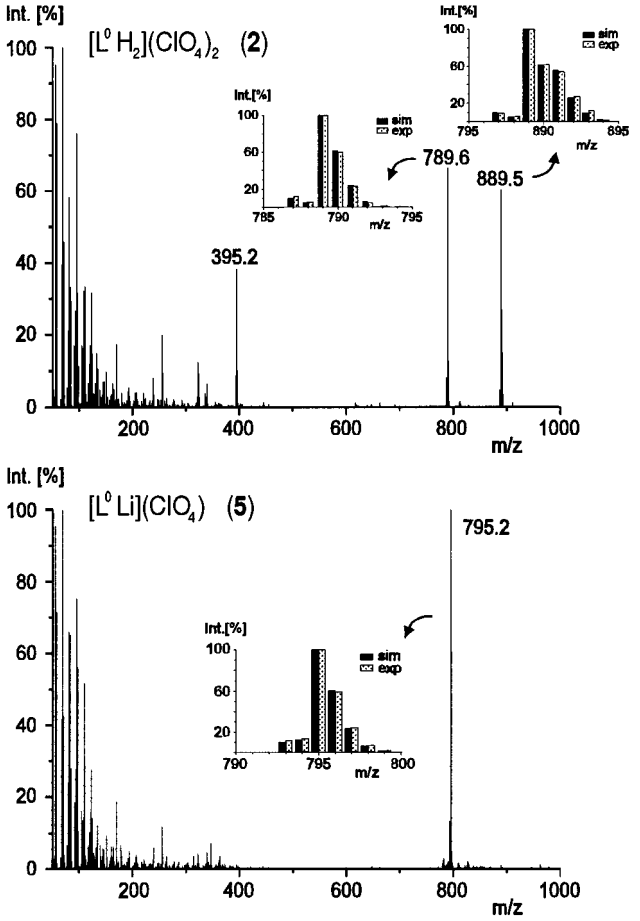


**Figure 1.** Positive-ion FAB mass spectra of $[L^0(H^+)_2](ClO_4)_2$ (**2**) and $[L^0Li]ClO_4$ (**5**). Matrix: *m*-nitrobenzyl alcohol.

the macrobicycle $L^0$. There is practically no indication in the spectrum for ligand fragmentation or cleavage of the dimer, except a small amount of dissociation of the tridentate amine, 1,4,7-trimethyl-1,4,7-triazacyclononane (L) (4% in **1** and 7% in **2**) from the corresponding most abundant species $[L^0(H^+)]^+$ in **1** and **2**. There must be a particularly strong driving force for $H^+$ incorporation, because even **3**, $L^0$, yields peaks at *m*/*z* 789 and 395, corresponding to the monocharged $[L^0(H^+)]^+$ and doubly charged $[L^0(H^+)_2]^{2+}$ species, respectively, with strong intensities. Interestingly, no peak for the species $[L^0(H^+)_4(ClO_4)_3]^+$, not even from the tetraprotonated complex **4**, could be observed, presumably due to its strong acidic character.

The mass spectra generally of these complexes and particularly that of **5**, $[L^0(Li)](ClO_4)$, have only a few peaks in the

(26) Lever, A. B. P. *Inorganic Electronic Spectroscopy*; Elsevier: Amsterdam, 1984.
(27) McCarthy, P. J.; Güdel, H. U. *Coord. Chem. Rev.* **1988**, *88*, 69.
(28) Krumholz, P. *Struct. Bonding (Berlin)* **1971**, *9*, 139.
(29) Panda, R. K.; Acharya, S.; Neogi, G.; Ramaswamy, D. *J. Chem. Soc., Dalton Trans.* **1983**, 1225.
(30) (a) Cetini, G.; Operti, L.; Vaglio, G. A.; Peruzzini, M.; Stoppioni, P. *Polyhedron* **1987**, *6*, 1491. (b) Bojesen, G. *Org. Mass Spectrom.* **1985**, *20*, 413. (c) Whiteford, J. A.; Rachlin, E. M.; Stang, P. J. *Angew. Chem.* **1996**, *108*, 2643. (d) Losada, G.; Mendiola, M. A.; Sevilla, M. T. *Inorg. Chim. Acta* **1997**, *255*, 125.

**Table 3.** Cyclic Voltammetric Data for the Complexes

| complex | oxidations[a] $E_{1/2}^{ox}$ or $E_p^{ox}$/V vs NHE | | reductions[a] $E_{1/2}^{red}$ or $E_p^{red}$/V vs NHE | |
|---|---|---|---|---|
| **2**, $Cr^{III}(H^+)_2Cr^{III}$ | +1.69 (ir) | +1.1 (ir) | | −1.61 (ir) |
| **7**, $Cr^{III}Cu^{II}Cr^{III}$ | +1.43 (qr) | +1.02 (qr) | −0.85 (qr) | |
| **8**, $Cr^{III}Ni^{II}Cr^{III}$ | +1.32 (r) | +0.89 (r) | | −1.65 (qr) |
| **10**, $Cr^{III}Co^{III}Cr^{III}$ | | | −0.35 (r) | −1.14 (r) |
| **11**, $Cr^{III}Fe^{II}Cr^{III}$ | | +0.53 (r) | | −1.86 (qr) |
| **13**, $Cr^{III}Mn^{II}Cr^{III}$ | +1.3 (qr) | +0.57 (qr) | | 1.63 (qr) |

[a] r = reversible, $\Delta E_p$ = 65−70 mV; qr = quasi-reversible, $\Delta E_p$ = 70−140 mV; $E_{1/2} = (E_p^{ox} + E_p^{red})/2$; ir = irreversible. Electrochemical reversibility and quasi-reversibility were judged on the basis of standard criteria described in the literature; see, e.g.: (a) Nicholson, R. S.; Shain, I. *Anal. Chem.* **1964**, *36*, 706. (b) Bard, A. J.; Faulkner, L. R. *Electrochemical Methods: Fundamentals and Applications*; Wiley: New York, 1980. Conditions: acetonitrile solution; 0.10 M $(Bu_4N)PF_6$ supporting electrolyte; glassy carbon working electrode; Ag/AgCl (saturated LiCl in $C_2H_5OH$) reference electrode; ferrocene (~$10^{-3}$ M) as internal standard; scan rates 20−200 mV $s^{-1}$; room temperature.

higher mass region, as is illustrated by Figure 1, and they are easily assigned to the cationic complex, clusters of the complex with the counteranion, and free (protonated) ligand. The inserts in Figure 1 illustrate that the resolution is sufficient to determine the formal charge of the complex cations and provide a check of the isotopic patterns. Figure 1 with $[L^0(Li)]^+$ as the base peak supplies clear-cut evidence for the composition of the novel Li complex, **5**, with the macrobicycle, **3**. It should be noted that a peak for the respective complex cation is observed in the spectra of all complexes (Table 2).

The mass spectra of complexes **11** and **12** exhibit identical ions, although they contain iron in different oxidation states; such behavior has been ascribed to the interactions that occur between the samples and the matrix containing the reducing alcohol group. Complex **12** containing a ferric central ion is an oxidizing agent, as is evident from the redox potential measured by the electrochemical measurements; it undergoes a fast redox reaction, with the matrix *m*-nitrobenzyl alcohol prior to forming ions in the gas phase, to produce complex **11** with a ferrous ion and, hence, gives same mass spectrum as that of **11**.

To conclude, the data summarized in Table 2 show that the mass spectrometry of the complexes unambiguously demonstrate the nuclearity of all the complexes examined and also provide identification of the metal centers and, in general, the composition of the complexes. It seems that the complexes **1**−**13** are not fragile and can withstand the conditions of the L-SIMS ionization.[31]

**Electrochemistry.** The cyclic voltammograms (CV) of complexes **2**−**13** were measured at ambient temperature in $CH_3CN$ containing 0.1 M tetra-*n*-butylammonium hexafluorophosphate as supporting electrolyte at a glassy carbon working electrode at different scan rates. The results of electrochemistry are summarized in Table 3 and Figure 2. All redox potentials in the following are referenced in volts versus NHE, considering the potential of the ferrocenium/ferrocene couple, used as an internal standard, to be 0.4 V vs NHE.

Two irreversible electron-transfer waves are detected in the potential range +1.9 to 0.0 V at $E_1^{ox}$ = +1.11 V and $E_2^{ox}$ = +1.71 V for **2**. The first process $E_1^{ox}$ corresponds to the Cr(IV)/Cr(III) couple, followed by decomposition of the oxidized Cr(IV) form. The assignment of metal-centered oxidation at $E_1^{ox}$ is supported by comparison with the CV of $Cr^{III}Zn^{II}Cr^{III}$. The

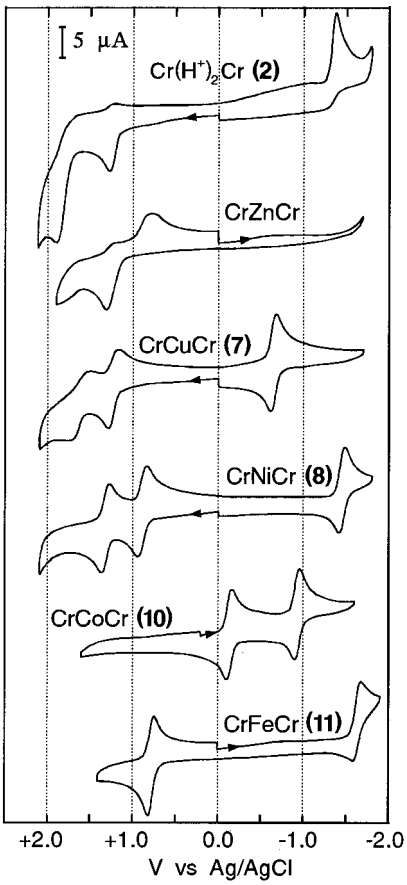


**Figure 2.** Cyclic voltammograms of **2**, **7**, **8**, **10**, and **11** in $CH_3CN$ at a scan rate of 0.2 V $s^{-1}$.

second process, $E_2^{ox}$, has been tentatively assigned to the ligand dimethylglyoxime rather than metal-centered electron transfer wave. Considering nearly identical electronic situation for the terminal $CrN_3O_3$ units in both **2** and $Cr^{III}Zn^{II}Cr^{III}$ and the observation of one irreversible reduction at −1.59 V only in **2**, but not in $Cr^{III}Zn^{II}Cr^{III}$, this reduction in **2** is assigned to the ligand dimethylglyoxime rather than the chromium(III)-centered electron transfer.

The central $Cu^{II}$ of **7** in a $CuN_6$ environment is quasi-reversibly oxidized to $Cu^{III}$ at +1.04 V and to $Cu^{IV}$ at +1.45 V. Thus ligand-centered oxidation is not observed for **7**. At the same potential of +1.45 V, a one-electron reversible oxidation for the $Cr^{III}Cu^{II}Cr^{III}$ complex with diphenylglyoxime[32] as the dioxime ligand is observed, which is in complete accord with the assignment, $Cu^{IV}/Cu^{III}$ couple, for **7**. In negative potential range **7** shows one quasi-reversible one-electron-transfer wave at −0.83 V, which is assigned to the Cu(II)/Cu(I) couple. A similar electrochemical process has been observed for $Cu(Hdmg))_2$.[33]

Two consecutive reversible steps of oxidation in the potential range 0.0 to +1.5 V at $E_{1/2}^{ox1}$ = +0.70 V and $E_{1/2}^{ox2}$ = +1.13 V are detected for **8**, $Cr^{III}Ni^{II}Cr^{III}$. Thus the following redox scheme, involving the oxidation of central $Ni^{II}$ ion in **8**, is ascribed to the electrochemical oxidation processes for complex **8**:

$$Cr^{III}Ni^{II}Cr^{III} \overset{E_{1/2}^{ox1}}{\rightleftharpoons} Cr^{III}Ni^{III}Cr^{III} \overset{E_{1/2}^{ox2}}{\rightleftharpoons} Cr^{III}Ni^{IV}Cr^{III}$$

Electrochemical reversible one-electron transfer steps (1e

(31) (a) McNeal, C. J. *Anal. Chem.* **1982**, *54*, 43A. (b) Barber, M.; Bordoli, R. S.; Elliott, G. J.; Sedgwick, R. D.; Tyler, A. N. *Anal. Chem.* **1982**, *54*, 645A.

(32) (a) Birkelbach, F. Dissertation, Bochum, 1995. (b) Burdinski, D. Diploma Thesis, Bochum, 1995.

transfer established by coulometric experiments) preclude any significant structural rearrangement during the oxidation processes; i.e., all three species have the same structures in solution and apparently can be described by the solid-state structure of **8**, $Cr^{III}Ni^{II}Cr^{III}$, which was determined by X-ray diffraction. The CV of the isolated stable oxidation product $Cr^{III}Ni^{IV}Cr^{III}$ (**9**) is identical with that of **8**. A very similar electrochemical oxidation process has been reported[3] for analogous $Fe^{III}Ni^{II}$-$Fe^{III}$. A quasi-reversible reduction at −1.63 V is also observed for **8**, which cannot be unambiguously ascribed to the nickel center, as several Ni(II)-stabilized ligand radicals with α-diimines are known in the literature.[34] This reduction may therefore be ligand centered in nature.

The CV of **10**, $Cr^{III}Co^{III}Cr^{III}$, is also shown in Figure 2. Two reversible one-electron transfer waves are detectable at $E_{1/2}^{red1} = -0.33$ V and $E_{1/2}^{red2} = -1.12$ V, which can be assigned to the following equilibria:

$$Cr^{III}Co^{III}Cr^{III} \overset{E_{1/2}^{red1}}{\rightleftharpoons} Cr^{III}Co^{II}Cr^{III} \overset{E_{1/2}^{red2}}{\rightleftharpoons} Cr^{III}Co^{I}Cr^{III}$$

Both the reduced species are, however, stable only in the cyclic voltammetric time scale, as is evidenced by the coulometric experiments at −0.5 V vs Ag/AgCl (current yield > 130%). Contrary to **10**, the comparable B-capped cobalt−dimethylglyoxime complex is isolable in both $[Co^{III}(dmg)_3(BF)_2]$ and $[Co^{II}(dmg)_3(BF)_2]^-$ forms.[12]

Replacement of the central $Co^{III}$ in **10** by $Fe^{II}$ gives the dicationic complex **11**, which shows two one-electron transfer waves: one reversible oxidation at +0.59 V and one quasi-reversible reduction at −1.82 V. The former event is assigned to the Fe(III)/Fe(II) couple. In the literature[15,35] there are several reports of the electrochemical oxidation of tris(dioxime)iron(II) to the corresponding Fe(III) form, but none of the Fe(III) complexes could be isolated, because of their instability. A coulometric experiment at +1.0 V vs Ag/AgCl for **11** established the stability (current yield = 96%) of the tris(dimethylglyoximato)iron(III) unit and showed its accessibility; in fact, $Cr^{III}Fe^{III}(ls)Cr^{III}$ (**12**) has been isolated as a brown microcrystalline solid. The reduction wave might be due to the involvement of the Fe(II)/Fe(I) couple. Again, we cannot preclude ligand-centered electron transfer. From an acetonitrile solution of **12**, an identical CV has been obtained.

The cyclic voltammetric behavior of **13**, $Cr^{III}Mn^{II}Cr^{III}$, shows two quasi-reversible one-electron oxidations at +0.59 and +1.32 V vs NHE, tentatively assigned to the Mn(III)/Mn(II) and Mn(IV)/Mn(III) couples, respectively. An irreversible reduction at −1.61 V, followed by a small oxidation wave at −1.09 V, is again attributable to the ligand reduction.

**Description of the Structures. Molecular Structure of $[L^0(H^+)_2](ClO_4)_2 \cdot CH_3OH$ (2).** The structure has been reported in a previous publication.[20]

**Molecular Structure of $[L^0(Cu^{II})](ClO_4)_2 \cdot CH_3OH$ (7).** Figure 3 displays the structure of the dication in **7**. The X-ray structure clearly illustrates the trinuclear nature of the cation. The bond lengths of the $N_3Cr(O\text{-}N)_3Cu\text{-}(N\text{-}O)_3CrN_3$ core in **7** are given in Table 4. The $[Cu(dmg)_3]^{4-}$ anion bridges two terminal Cr(III) ions through its deprotonated oxime oxygens with a Cr···Cu separation of 3.583(2) Å. The trinuclear Cr−Cu−Cr unit is not perfectly linear with an angle of 175.1°. Two facially coordinated tridentate amine ligands complete the trigonally distorted octahedral coordination sphere of the two Cr(III) centers. The Cr−N (average 2.128(7) Å) and Cr−O (average 1.920(5) Å) distances are comparable to literature[2,37] values for chromium(III) complexes with this macrocyclic amine.

The Cu−N distances and the twist angles (Table 5) show that the resultant coordination sphere around the disordered Cu is strongly distorted. The six imine-nitrogen atoms are arranged around the Cu(II) center with two different twist angles of 6.4 and 9.4° between the triangular faces comprising the oxime-nitrogens. The Cu atom is thus displaced from the center of the complex and closer to two of the bridging dimethylglyoximate ligands; the distance to the third oxime ligand is remarkably long. The geometry of the Cu center may be envisaged as pseudo-square pyramidal with an $\eta^2$-dmg ligand at the apical position and is very similar to that found in the corresponding $Fe^{III}Cu^{II}Fe^{III}$ compound.[9]

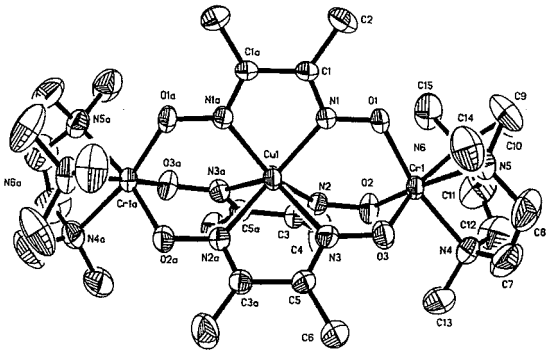


**Figure 3.** ORTEP diagram of the dication $[L_2Cr_2(dmg)_3Cu]^{2+}$ in **7**.

**Table 4.** Selected Bond Distances for Complexes $Cr^{III}Cu^{II}Cr^{III}$ (**7**), $Cr^{III}Ni^{II}Cr^{III}$ (**8**), and $Cr^{III}Fe^{II}Cr^{III}$ (**11**)

| | | distance, Å | | |
|---|---|---|---|---|
| | $Cr_2Zn$[a] | $Cr_2Cu$ (**7**) | $Cr_2Ni$ (**8**) | $Cr_2Fe$ (**11**) |
| M(II)−N(1) | 2.131(5) | 1.997(4) | 2.067(2) | 1.943(3) |
| M(II)−N(2) | 2.178(7) | 2.147(4) | 2.072(2) | 1.937(3) |
| M(II)−N(3) | 2.138(7) | 2.229(4) | 2.058(2) | 1.929(3) |
| Cr(III)−N(4) | 2.129(8) | 2.122(4) | 2.126(2) | 2.124(3) |
| Cr(III)−N(5) | 2.123(8) | 2.129(4) | 2.122(2) | 2.119(3) |
| Cr(III)−N(6) | 2.126(6) | 2.134(4) | 2.121(2) | 2.121(3) |
| Cr(III)−O(1) | 1.922(6) | 1.919(3) | 1.940(2) | 1.945(2) |
| Cr(III)−O(2) | 1.936(4) | 1.916(3) | 1.946(1) | 1.934(2) |
| Cr(III)−O(3) | 1.911(6) | 1.925(3) | 1.945(2) | 1.940(2) |

[a] Reference 32; listed here for comparison purpose.

**Table 5.** Comparison of Important Structural Parameters for Complexes **2**, **7**, **8**, **11**, and $Cr^{III}Zn^{II}Cr^{III}$ [b]

| | complex | $Cr^{III}\cdots Cr^{III}$, Å | $Cr^{III}\cdots M^{II}$, Å | ∠CrMCr, deg | twist angle, $\phi$, deg |
|---|---|---|---|---|---|
| **2**, | $Cr^{III}(H^+)_2Cr^{III}$ [a] | 7.265 | | | 0.5/8.4/8.4 |
| | $Cr^{III}Zn^{II}Cr^{III}$ [b] | 7.140 | 3.570 | 179.7 | 6.1/7.4/7.4 |
| **7**, | $Cr^{III}Cu^{II}Cr^{III}$ | 7.160 | 3.583 | 175.1 | 6.4/9.4/9.4 |
| **8**, | $Cr^{III}Ni^{II}Cr^{III}$ | 7.063 | 3.532 | 179.0 | 24.8/23.3/23.3 |
| **11**, | $Cr^{III}Fe^{II}Cr^{III}$ | 6.933 | 3.467 | 178.6 | 36.6/33.9/33.9 |

[a] Reference 20. [b] Reference 32.

(33) Chaudhuri, P.; Winter, M.; Della Vedova, B. P. C.; Bill, E.; Trautwein, A. X.; Gehring, S.; Fleischhauer, P.; Nuber, B.; Weiss, J. *Inorg. Chem.* **1991**, *30*, 2148.
(34) (a) Nag, K.; Chakravorty, A. *Coord. Chem. Rev.* **1980**, *33*, 87. (b) Lappin, A. G.; McAuley, A. *Adv. Inorg. Chem.* **1988**, *32*, 241.
(35) Grzybowski, J. J.; Allen, R. D.; Belinski, J. A.; Bieda, K. L.; Bish, T. A.; Finnegan, P. A.; Hartenstein, M. L.; Regitz, C. S.; Ryalls, D. M.; Squires, M. E.; Thomas, H. J. *Inorg. Chem.* **1993**, *32*, 5266.
(36) Chaudhuri, P.; Winter, M.; Birkelbach, F.; Fleischhauer, P.; Haase, W.; Flörke, U.; Haupt, H.-J. *Inorg. Chem.* **1991**, *30*, 4291.
(37) Chaudhuri, P.; Wieghardt, K. *Prog. Inorg. Chem.* **1987**, *35*, 329.
(38) See for example: Morehouse, S. M.; Polychronopoulou, A.; Williams, G. J. B. *Inorg. Chem.* **1980**, *19*, 3558.

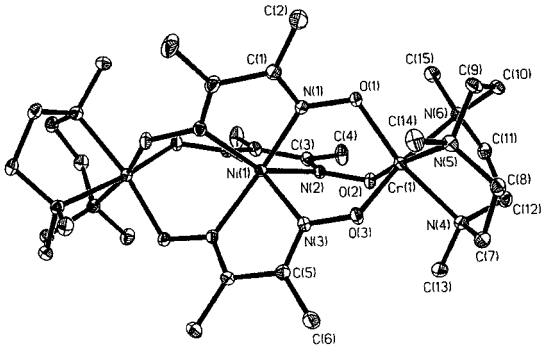


**Figure 4.** Molecular structure of the dication $[L_2Cr_2(dmg)_3Ni]^{2+}$ in **8**.

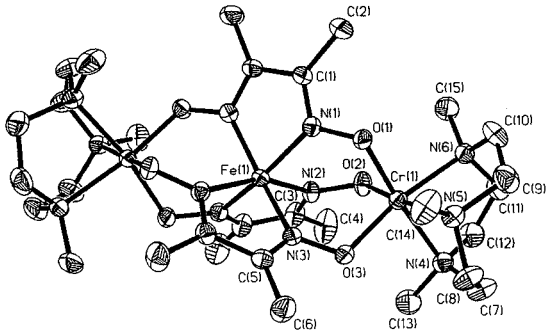


**Figure 5.** Structure of the dication $[L_2Cr_2(dmg)_3Fe(ls)]^{2+}$ in crystals of **11**.

**Molecular Structures of $[L^0(Ni^{II})](ClO_4)_2$ (8) and $[L^0(Fe^{II})](ClO_4)_2 \cdot H_2O$ (11).** The structures of the dications in **8**, $Cr^{III}Ni^{II}Cr^{III}$, and in **11**, $Cr^{III}Fe^{II}Cr^{III}$, are very similar to that of the dication in **7** (Figures 4 and 5). The Cr−N bond distances in **8** and **11** are identical within experimental errors to those of **7** and $Cr^{III}Zn^{II}Cr^{III}$. It is quite remarkable and significant that the Cr−O distances in **8** and **11** are very similar, but they are significantly longer than those in **7** and $Cr^{III}Zn^{II}Cr^{III}$ (Table 4).

The mean Ni−N(oxime) bond length for **8**, 2.065(7) Å, is identical within experimental errors with that for a related Ni(II) derivative, 2.030(21) Å, of the bicyclic clathrochelate ligand $[FB(ONCHC_5H_3N)_3P]^-$, described by Holm and co-workers,[13b,39] but is appreciably longer than that found in $Ni(Hdmg)_2$, 1.850(15) Å,[40] in accordance with the greater steric requirements in the central $Ni(dmg)_3$ unit. The trigonal twist angle (0° for a trigonal prismatic arrangement and 60° for an octahedron or trigonal-antiprismatic) is ∼24° for Ni(II) (Table 5).

Of the available $Cr^{III}M^{II}Cr^{III}$ species, the $d^6$ low-spin Fe(II) species, **11**, is most likely to distort from $D_{3h}$ symmetry, both for reasons of inherent ligand-field stabilization energy, LFSE (which is a maximal 24*Dq* for an octahedral strong-field $d^6$ ion) and for steric reasons, since the $Fe^{2+}$ ion is the smallest (0.75 Å) of the quintet $Mn^{2+}$ (0.97 Å), $Fe^{2+}$ (0.75 Å), $Ni^{2+}$ (0.83 Å), $Cu^{2+}$ (0.87 Å), and $Zn^{2+}$ (0.88 Å).[41] The average Fe−N(oxime) bond length, 1.936(7) Å, in **11** is in accord with a $d^6$ low-spin electronic configuration and is very similar to that of a related FB-capped clathrochelate.[42] The twist angle between the two equilateral triangles defined by the oxime nitrogens are 36.6, 33.9, and 33.9°, thus averaging to 34.8°. The coordination environment of the iron atom is thus intermediate between trigonal prismatic and octahedral.[15a,43]

The principal difference in interatomic parameters involves the systematic decrease of M−N bond lengths within the $MN_6$ coordination sphere in the order Zn > Cu > Ni ≫ Fe (Table 4). The differences between M(II)−N distance and $M^{2+}$ radii are 1.269 Å for Zn(II), 1.254 Å for Cu(II) (**7**), 1.236 Å for Ni(II) (**8**), and 1.186 Å for Fe(II) (**11**); i.e., there is a small but nonnegligible variation in the metal−nitrogen bond distances.

All of the structural data are consistent with the geometry of the central metal coordination sphere being determined not only by the relative sizes of the metal atom and the cavity within the bicyclic encapsulation ligand but also by the ligand-field effects. The Fe(II) atom is clearly too small to fit into the cavity without causing a severe distortion toward an octahedral geometry. Electronic effects (LFSE) also favor for the low-spin $d^6$ ion, Fe(II), an octahedral environment. Thus both of these factors, electronic and size effects, are responsible for the geometrical distortions found in these trinuclear complexes. That the twist angles for complexes containing Mn(II) and Zn(II) as central metal ions are very similar has been observed for the related trimetallic complexes with Fe(III) and Mn(III) as terminal metal ions.[10] The twist angle for **2** (Table 5) indicates that the unprotonated dinuclear macrobicycle **3**, $L^0$, possesses very close to ideal $D_{3h}$ symmetry. While the order of stability for octahedral geometry as a function of LFSE is ls-Fe(II) ≫ Ni(II) > Cu(II) > hs-Mn(II) = Zn(II), it must be emphasized that LFSE effects are more important to ligand systems with a flexible geometry than to the present rather rigid cage structure.

**Mössbauer Spectroscopic Properties.**[48] The Mössbauer spectra of $Cr^{III}Fe^{II}Cr^{III}$ (**11**) and $Cr^{III}Fe^{III}Cr^{III}$ (**12**) were measured at 77 and 295 K, respectively, to determine the spin and oxidation states of the central iron. The Mössbauer parameters of **11** ($\delta = 0.23$ mm/s, $\Delta E_Q = 0.16$ mm/s) clearly indicate the low-spin nature of the Fe(II) ion. The Mössbauer spectrum of **12** at 295 K consists of a symmetric quadrupole doublet with an isomer shift of $\delta_Q = 0.073$ mm/s and a quadrupole splitting of $\Delta E_Q = 0.96$ mm/s. The relatively small value for the isomer shift together with the substantially greater quadrupole splitting in comparison to that of **11** are indicative of low-spin Fe(III), consistent with the magnetic results described later.

**Magnetic Susceptibility Studies.** Magnetic susceptibility data for polycrystalline samples of complexes **1**−**13** (except for **3**, **6**, and **9**) were collected in the temperature range 2−295 K in order to characterize the nature and magnitude of the exchange interaction propagated by the bridging oxime ligands. We use the Heisenberg spin Hamiltonian in the form

$$H = -2J(S_1 \cdot S_2 + S_2 \cdot S_3) - 2J_{13}(S_1 \cdot S_3)$$

for an isotropic exchange coupling with $S_1 = S_3 = S_{Cr} = {}^3/_2$ and $S_2 = S_M = 0$ for $(H^+)_2$, **1**, **2**, and $(H^+)_4$ (**4**), Li(I) (**5**), Co(III) (**10**), and Fe(II) (**11**), $S_2 = S_M = {}^1/_2$ for Cu(II) (**7**), Fe(III,ls) (**12**), $S_2 = S_M = 1$ for Ni(II) (**8**), or $S_2 = S_M = {}^5/_2$ for Mn(II) (**13**), with a negative "*J*" value corresponding to an antiferromagnetic interaction and a positive "*J*" value to a ferromagnetic coupling. The experimental magnetic data were simulated using a least-squares fitting computer program with a full-matrix diagonalization approach including exchange coupling, Zeeman splitting, and single-ion zero-field interactions ($DS_z^2$), if neces-

(39) Churchill, M. R.; Reis, A. H. *Inorg. Chem.* **1972**, *11*, 1811.
(40) (a) Godycki, L. E.; Rundle, R. E. *Acta Crystallogr.* **1953**, *6*, 487. (b) Williams, D. E.; Wohlauer, G.; Rundle, R. E. *J. Am. Chem. Soc.* **1959**, *81*, 755.
(41) Cotton, F. A.; Wilkinson, G. *Advanced Inorganic Chemistry*; John Wiley & Sons: New York, 1988.
(42) (a) Churchill, M. R.; Reis, A. H. *Inorg. Chem.* **1972**, *11*, 2299. (b) Lindeman, S. V.; Struchkov, Y. T.; Voloshin, Y. Z. *Inorg. Chim. Acta* **1991**, *184*, 107.
(43) (a) Wentworth, R. A. D. *Coord. Chem. Rev.* **1972/73**, *9*, 171. (b) Kirchner, R. M.; Mealli, C.; Bailey, M.; Howe, N.; Torre, L. P.; Wilson, L. J.; Andrews, L. C.; Rose, N. J.; Lingafelter, E. C. *Coord. Chem. Rev.* **1987**, *77*, 89.

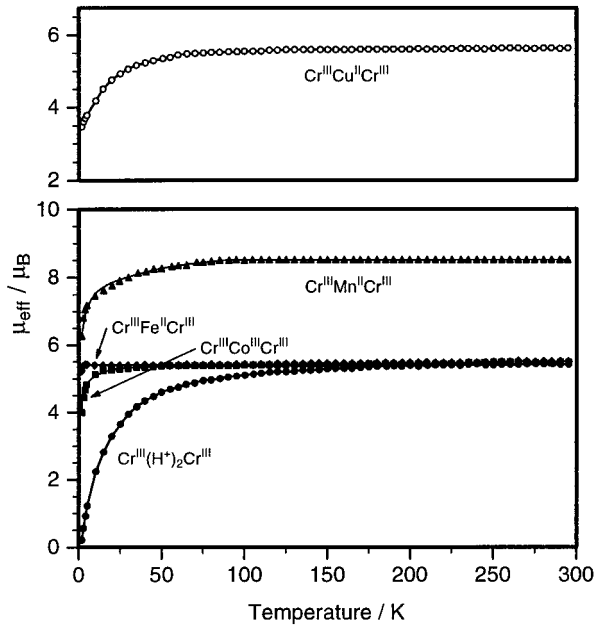


**Figure 6.** Temperature dependence of the magnetic moments of complexes **1**, **7**, **10**, **11**, and **13**. The solid lines represent the best fit of data to the Heisenberg−Dirac−van Vleck model (see text).

**Table 6.** Magnetic Data for the Dinuclear and Trinuclear Complexes

| complex | $J$/cm$^{-1}$ ($J_{12} = J_{23}$) | $J_{13}$/cm$^{-1}$ | $\langle g \rangle$ |
|---|---|---|---|
| **1**, $[Cr^{III}(H^+)_2Cr^{III}]Br_2$ | | −5.1 | 1.91 |
| **2**, $[Cr^{III}(H^+)_2Cr^{III}](ClO_4)_2$ | | −4.7 | 2.04 |
| **4**, $Cr^{III}(H^+)_4Cr^{III}$ | | −3.1 | 2.04 |
| **5**, $Cr^{III}Li^{I}Cr^{III}$ | | −5.8 | 2.07 |
| **7**, $Cr^{III}Cu^{II}Cr^{III}$ | +18.5 | −7.0 | 1.96 |
| **8**, $Cr^{III}Ni^{II}Cr^{III}$ | −0.7 | −1.8 | $g_{Cr} = 2.0$, $g_{Ni} = 2.15$ |
| **10**, $Cr^{III}Co^{III}(ls)Cr^{III}$ | | −0.3 | 1.99 |
| **11**, $Cr^{III}Fe^{II}(ls)Cr^{III}$ | | 0 | 1.98 |
| **12**, $Cr^{III}Fe^{III}(ls)Cr^{III}$ | −15.7 | −3.0 | 1.99 |
| **13**, $Cr^{III}Mn^{II}Cr^{III}$ | +4.5 | −11.5 | 2.06 |

sary. In our model $J$ ($=J_{12} = J_{23}$) represents the exchange interaction between adjacent metal ions, i.e., the terminal chromium and the central divalent or trivalent metal ions, whereas $J_{13}$ describes the interaction between the terminal chromium nuclei within the trinuclear complex. Table 6 summarily presents the intramolecular exchange parameters.

As the complexes **1**, **2**, **4**, **5**, **10**, and **11** containing only two paramagnetic centers, viz. Cr(III), may be considered magnetically as dinuclear complexes, we start our discussion with their magnetic properties. The temperature dependence of the magnetic moments of the "dinuclear" complexes **1**, **10**, and **11** are displayed in Figure 6. In a preliminary report we have already published the temperature dependence of the magnetic susceptibility and magnetic moment for **2**.[20] **1** is the bromide salt of the cation in **2** and exhibits, as is expected, temperature dependence identical to that for **2**.

The magnetic moment $\mu_{eff}$/molecule for **10**, $Cr^{III}Co^{III}Cr^{III}$, remains nearly constant from 295 K (5.54 $\mu_B$) to 40 K (5.38 $\mu_B$), below which it starts to decrease very slowly with decreasing temperature until it reaches the value of 5.12 $\mu_B$ at 10 K. Below 10 K there is a rapid decrease in $\mu_{eff}$ reaching a value of 3.99 $\mu_B$ at 2 K. For **11**, $Cr^{III}Fe^{II}(ls)Cr^{III}$, the temperature dependence of $\mu_{eff}$ is even smaller; the values of $\mu_{eff}$/molecule are 5.49 $\mu_B$ at 295 K, 5.43 $\mu_B$ at 10 K, 5.39 $\mu_B$ at 3 K, and 5.25 $\mu_B$ at 2 K.

The exchange coupling constants for **1**, **2**, **4**, **5**, **10**, and **11**, evaluated by simulation of the magnetic data, are given in Table 6. It is noteworthy that the *intra*molecular exchange coupling is observed in **1**, **2**, **4**, and **5**, in which the chromium(III) centers are separated by a large distance of ca. 7.2 Å. Incorporation of low-spin $d^6$ Co(III) and Fe(II) in **10** and **11**, respectively, by substituting protons of $Cr^{III}(H^+)_2Cr^{III}$ (**1** and **2**), inhibits the exchange interaction ($J \approx 0$), demonstrating the different roles of the central diamagnetic ions on the magnitude of the magnetic interactions between the terminal chromium(III) centers separated by a distance of $\sim$ 7.2 Å. The above points are relevant for the exchange mechanism that will be discussed later.

The cryomagnetic property of the $Cr^{III}Cu^{II}Cr^{III}$ complex, **7**, is shown in Figure 6 in the form of a $\mu_{eff}$ vs $T$ plot. The magnetic moment of 5.64 $\mu_B$ at 295 K remains nearly constant until 100 K with a value of $\mu_{eff} = 5.57$ $\mu_B$. Below 100 K, the magnetic moment decreases very slowly to a value of 4.21 $\mu_B$ at 10 K and then it starts to decrease rapidly reaching a value of 3.51 $\mu_B$ at 2 K. The least-squares fitting, shown as the solid line in Figure 6, of the experimental data leads to $J = +18.5$ cm$^{-1}$, $J_{13} = -7.0$ cm$^{-1}$, and $g = 1.96$. Similar ferromagnetic coupling has been observed for the bis(oximato)-bridged $Cr^{III}$-$Cu^{II}$ species.[5,44] Interestingly, the strength of the ferromagnetic coupling in **7** is identical with that in a $Cr^{III}Cu^{II}$ dinuclear compound, described earlier.[5] **7** is the first structurally characterized tris(oximato)-bridged $Cr^{III}Cu^{II}Cr^{III}$ trinuclear compound, and the parallel spin coupling ($J = +18.5$ cm$^{-1}$) between the neighboring Cr(III) and Cu(II) ions falls at the upper end of the observed range for all similar compounds known in the literature.[44,45] It is interesting to note that the related isoelectronic $Mn^{IV}Cu^{II}Mn^{IV}$ complex also exhibits ferromagnetism, but the exchange interaction is remarkably stronger ($J = +72.7$ cm$^{-1}$),[10] attributable to the higher charge on the Mn(IV) center than that on the Cr(III) center. Thus, the higher covalent character of the Mn(IV)-ligand bond leads to stronger electronic interactions. The nearest-neighbor interaction, $J$, is ferromagnetic, while $J_{13}$ is antiferromagnetic for **7**. Because of the competing influence of $J$ and $J_{13}$ upon spin coupling in **7**, the ground-state possesses an $S_t = {}^3/_2$, which lies 4.5 and 9.5 cm$^{-1}$ below the first excited state with $S_t = {}^1/_2$ and the second excited state with $S_t = {}^5/_2$, respectively. If one neglects the terminal coupling $J_{13}$, the ground state of **7** would be $S_t = {}^7/_2$. The energy ladders for **7** evaluated with and without $J_{13}$ are depicted in Figure 7. Similar ground-state variability, i.e., the influence of $J_{13}$ on the spin ladder, has been unambiguously demonstrated earlier by us.[10] It is known[8a] that the ground state is determined not by the absolute values of $J$ and $J_{13}$ but by their ratio $J_{13}/J$.

It is necessary to mention here that, on replacing dimethylglyoxime by diphenylglyoxime (dpg) in the corresponding $Cr^{III}$-$Cu^{II}Cr^{III}$(dpg) complex, the exchange coupling constants of $J = +4.7$ cm$^{-1}$ and $J_{13} = -5.3$ cm$^{-1}$ lead to a ratio of $J_{13}/J = -1.13$, and as a result of that, the ground state changes to $S_t = {}^1/_2$ for the $Cr^{III}Cu^{II}Cr^{III}$(dpg) complex.[21,32] The diphenylglyoxime series will be reported in detail in a forthcoming paper. The energy ladder for the diphenylglyoxime complex is also shown in Figure 7 for the purpose of comparison. We want to

(44) (a) Zhang, S. W.; Liao, D.-Z.; Jiang, Z.-H.; Wang, G.-L. *Transition Met. Chem.* **1995**, *20*, 396. (b) Zhong, Z. J.; Okawa, H.; Matsumoto, N.; Sakiyama, H.; Kida, S. *J. Chem. Soc., Dalton Trans.* **1991**, 497.

(45) (a) Glerup, J.; Goodson, P. A.; Hodgson, D. J.; Lynn, M. H.; Michelsen, K. *Inorg. Chem.* **1992**, *31*, 4785. (b) Zhong, Z. J.; Matsumoto, N.; Okawa, H., Kida, S. *Inorg. Chem.* **1991**, *30*, 436. (c) Journaux, Y.; Kahn, O.; Zarembowitch, J.; Galy, J.; Jaud, J. *J. Am. Chem. Soc.* **1983**, *105*, 7585. (d) Andruh, M.; Melanson, R.; Stager, C. V.; Rochon, F. D. *Inorg. Chim. Acta* **1996**, *251*, 309. (e) Ohba, M.; Tamaki, H.; Matsumoto, N.; Okawa, H. *Inorg. Chem.* **1993**, *32*, 5385.

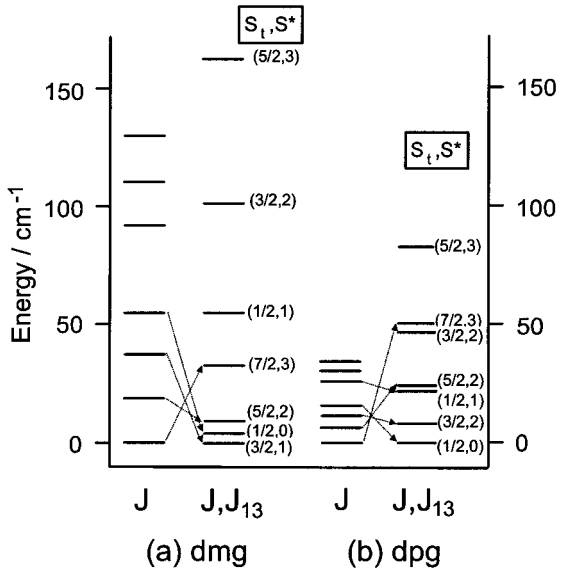


**Figure 7.** (a) Low-lying energy states for complex **7**, $Cr^{III}Cu^{II}Cr^{III}$(dmg), using $J$ and $J_{13}$ (levels on the right) and only $J$ (left-hand side) to show the effect of $J_{13}$ on the energy-splitting pattern. The corresponding change in the energy levels of the different states has been denoted by dotted arrows. The energy of the ground state $|S_t,S^*\rangle$ has arbitrarily been set at 0 $cm^{-1}$. (b) Spin ladder appropriate for the compound $Cr^{III}Cu^{II}Cr^{III}$(dpg), where dpg denotes the dioxime diphenylglyoxime.

emphasize here that two different exchange interactions are operative in these linear oximato-bridged trinuclear complexes. *The assumption occasionally made that no coupling prevails between the terminal ions may yield a wrong spin ground state.*

The magnetic moment, $\mu_{eff}$/molecule, for **8** changes only slightly from 6.19 $\mu_B$ at 290.3 K to 5.99 $\mu_B$ at 80 K. Below 80 K, $\mu_{eff}$ starts to decrease steadily reaching a value of 1.79 $\mu_B$ at 2 K (Figure 8). This magnetic behavior is quite characteristic of an antiferromagnetic coupling between the paramagnetic centers. To determine the zero-field parameter, particularly of the central Ni(II) ion, the magnetization as a function of $\beta H/kT$ at three different applied magnetic fields (1, 4, and 7 T) has been measured. The best fit for the three field-strengths yields the following parameters:

$$J = -0.70\ cm^{-1} \qquad J_{13} = -1.8\ cm^{-1} \qquad g_{Cr} = 2.00$$

$$g_{Ni} = 2.15 \qquad D_{Cr} = 1.0\ cm^{-1} \qquad D_{Ni} = 14.0\ cm^{-1}$$

We performed a systematic search in parameter spaces to determine the nature of the fit minimum. The error maps in fact reveal that the above parameters do represent a well-defined global minimum for this system. The correspondingly calculated (Figure 8, solid lines) $\chi_M$ and $\mu_{eff}$ vs $T$ curves with the above parameters show very good agreement with the experimental data. Thus we conclude that both of the interactions, neighboring and terminal, for **8**, $Cr^{III}Ni^{II}Cr^{III}$, are *antiferromagnetic* in nature. Interestingly, most of the known Cr(III)−Ni(II) interactions in the literature[46] are, in accord with the predictions made nearly 30 years ago,[47] ferromagnetic in nature.

The magnetic behavior of **12**, $Cr^{III}Fe^{III}$(ls)$Cr^{III}$, is also displayed in Figure 8. When the temperature is lowered $\mu_{eff}$ decreases monotonically from 5.50 $\mu_B$ at 300 K, approaches a broad minimum around 30 K ($\mu_{eff} \approx 4.79\ \mu_B$), and then starts

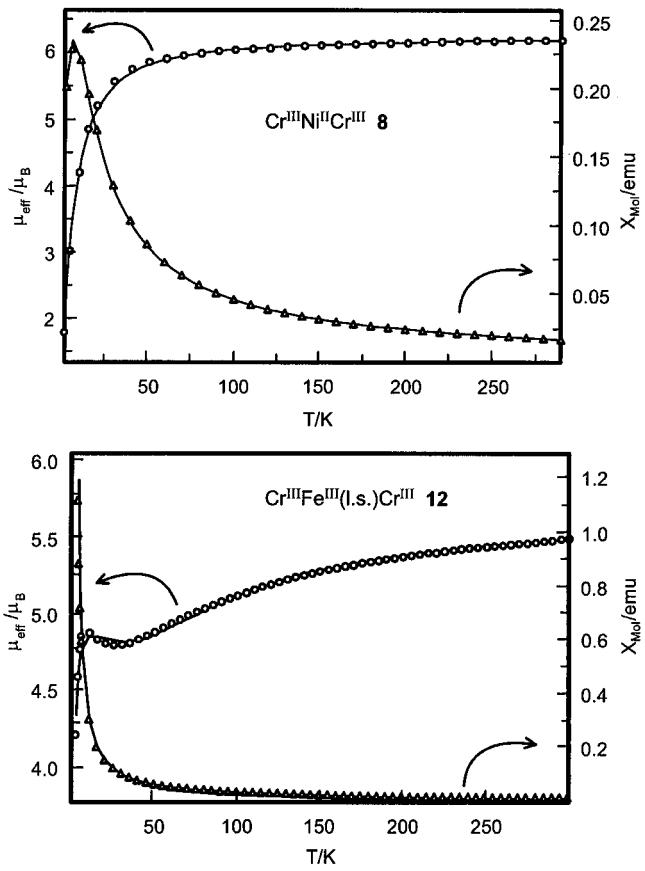


**Figure 8.** Plots of $\chi_M$ and $\mu_{eff}$ vs $T$ for solid **8** and **12**. The solid lines represent the best least-squares fits of the experimental data by the theoretical equation.

to decrease reaching a value of 4.21 $\mu_B$ at 2 K. The temperature behavior of the magnetic moment of **12** clearly indicates that $S = {}^1/_2$ of low-spin Fe(III) is antiferromagnetically coupled to the terminal $S = {}^3/_2$ of the Cr(III) ions. The least-squares fitting, shown as the solid line in Figure 8, yields $J = -15.7\ cm^{-1}$, $J_{13} = -3.0\ cm^{-1}$, and $g = 1.99$. It must be pointed out that the complex $Cr^{III}Cu^{II}Cr^{III}$, **7**, with the spin constellation of $S_1 = S_3 = {}^3/_2$ and $S_2 = {}^1/_2$ identical to that of **12**, $Cr^{III}Fe^{III}$(ls)$Cr^{III}$, exhibits parallel spin coupling between neighboring ions.

The magnetic moment for **13**, $Cr^{III}Mn^{II}Cr^{III}$, remains nearly constant (8.51−8.40 $\mu_B$) in the temperature range 295−70 K. Below 70 K it drops steadily and reaches a value of 6.23 $\mu_B$ at 2 K (Figure 6). A ferromagnetic coupling ($J = +4.5\ cm^{-1}$) between the neighboring $Cr^{III}$−$Mn^{II}$ and an antiferromagnetic interaction ($J_{13} = -11.5\ cm^{-1}$) between the terminal Cr(III) centers with an average $g = 2.06$ were evaluated by the fitting procedure. The $J_{13}$ value obtained from the fitting procedure for **13** is attached with a comparatively high error, as is evidenced by the error contour map showing a long minimum parallel to $J_{13}$ axis. But the error bar on the quoted $J$ value is small and can be estimated to be $\pm 0.5\ cm^{-1}$. Thus the $Cr^{III}$−

(46) (a) Pei, Y.; Journaux, Y.; Kahn, O. *Inorg. Chem.* **1989**, *28*, 100. (b) Corbin, K. M.; Glerup, J.; Hodgson, D. J.; Lynn, M. H.; Michelsen, K.; Nielsen, K. M. *Inorg. Chem.* **1993**, *32*, 18.

(47) (a) Martin, R. L. In *New Pathways in Inorganic Chemistry*; Ebsworth, Maddock, Sharpe, Eds.; Cambridge University Press: Cambridge, U.K., 1968; Chapter 9. (b) Ginsberg, A. P. *Inorg. Chim. Acta Rev.* **1971**, *5*, 45.

(48) (a) Gütlich, P.; Link, R.; Trautwein, A. *Mössbauer Spectroscopy and Transition Metal Chemistry*; Springer-Verlag: Berlin, Heidelberg, New York, 1978. (b) Gütlich, P. In *Mössbauer Spectroscopy*; Gonser, U., Ed.; Springer-Verlag: Berlin, 1975; Chapter 2.

**Scheme 2**

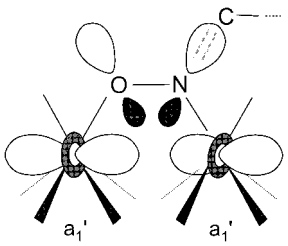


σ / π Superexchange

$Mn^{II}$ interaction in **13** is ferromagnetic like the corresponding $Mn^{IV}-Mn^{II}$ and $Mn^{III}-Mn^{II}$ interactions described earlier.[10] A very weakly ferromagnetically ($J = +0.5$ cm$^{-1}$) coupled oxalato-bridged $Cr^{III}Mn^{II}$ binuclear compound was recently reported, but without any X-ray structural characterization[45e].

**Concluding Discussion.** The trend in the sign and the magnitude of the neighboring spin-coupling in **7** ($Cr^{III}Cu^{II}Cr^{III}$), **8** ($Cr^{III}Ni^{II}Cr^{III}$), **12** ($Cr^{III}Fe^{III}$(ls)$Cr^{III}$), and **13** ($Cr^{III}Mn^{II}Cr^{III}$) can be qualitatively rationalized on the basis of the symmetry of the bridge-network, Cr(O-N)$_3$M, as a whole. The Cr(O-N)$_3$M heterobimetallic unit has an idealized $D_{3h}$ symmetry. The five metal d orbitals transform in $D_{3h}$ symmetry as $a'_1(d_{z^2})$, $e'(d_{x^2-y^2},d_{xy})$, and $e''(d_{xz},d_{yz})$. Thus, the following predominant exchange pathways can be envisaged for the Cr(III)−M pair, present in the complexes **7**, **8**, **12**, and **13**:

$$a'_1(d_{z^2})\|a'_1(d_{z^2}) \quad \text{antiparallel} \qquad (1)$$

$$a'_1(d_{z^2})\perp e'(d_{x^2-y^2},d_{xy}) \quad \text{parallel} \qquad (2)$$

$$a'_1(d_{z^2})\perp e''(d_{xz},d_{yz}) \quad \text{parallel} \qquad (3)$$

$$e'(d_{x^2-y^2},d_{xy})\|e'(d_{x^2-y^2},d_{xy}) \quad \text{antiparallel} \qquad (4)$$

$$e''(d_{xz},d_{yz})\|e''(d_{xz},d_{yz}) \quad \text{antiparallel} \qquad (5)$$

The sp$^2$-hybridized oxime (N and O atoms) ligand orbitals pointing toward the metal centers overlap most strongly with the $e''(d_{xz},d_{yz})$ metal d orbitals. The ligand orbitals, which are in the plane of the chelate ring, overlap most strongly with $a'_1(d_{z^2})$ of the metal d orbitals. It should be pointed out that the $a'_1a'_1$ overlap, shown in Scheme 2, is of both $\sigma$ and $\pi$ character. For the Cu(II) complex **7** ($d^3d^9d^3$), the unpaired electron of Cu(II) occupies the e′ orbital, which is the transformation of the $d_{x^2-y^2}$ and $d_{xy}$ orbitals in the $D_{3h}$ point group. As the antiferromagnetic path (1) is absent in **7**, the overall interaction observed in **7** is accordingly ferromagnetic.

If one next views the $Cr^{III}Ni^{II}Cr^{III}$ species, **8** ($d^3d^8d^3$), the ferromagnetic interaction ($J = +18.5$ cm$^{-1}$) decreases drastically to such an extent that a very weak antiparallel interaction ($J = -0.7$ cm$^{-1}$) is observed for the nickel complex, **8**. Thus, the contribution of the path (1), $J(a'_1a'_1)$, to the overall interaction is certainly very important, since the $a'_1$ orbitals centered both on chromium and nickel are situated in the plane of the bridging oxime network and interact efficiently. It should be noted that the local geometry of the central $NiN_6$ core is not perfectly trigonal prismatic but more twisted toward an octahedron with a twist angle of 23.8° than the corresponding $CuN_6$ core in **7**. This distortion from trigonal prismatic arrangement decreases the overlap between the magnetic orbitals of Cr(III) and Ni(II). Hence, the nature of the exchange interaction and its magnitude in triply bridged $Cr^{III}Ni^{II}$ pair is expected to be a function of the twist angle at the Ni center. The closer is the trigonal prismatic arrangement of the metal center, the stronger would be the antiferromagnetic interaction. We are working on this problem to establish this hypothesis.

For the $Cr^{III}Mn^{II}$ case, **13**, with the $d^3$(hs)$d^5$ electronic configuration, the experimental observation of a weaker parallel interaction (+4.5 cm$^{-1}$) than that in **7** shows that the antiparallel path (1) prevails, but the overall spin interaction is dominated by the parallel paths (2) and (3). Interestingly, occupancy of the e″ orbital by the single unpaired electron of Fe(III) in **12**, $d^3$(ls)$d^5$, results in an overall antiparallel spin coupling, showing the predominance of the superexchange path (5) in **12**.

The $\pi$-conjugated system of the oxime ligand, delocalized over the whole bridging groups and perpendicular to the plane of the oxime ligand, appears to provide the dominant antiferromagnetic interaction between the terminal Cr(III) ions, separated by as large as ∼7 Å. A comparison of the complexes containing a diamagnetic ion as the central species, i.e., **1**, **2**, **4**, **5**, **10**, and **11** (Table 6), clearly indicates the participation of the central metal ion in the transmission of the antiferromagnetic exchange interaction between the terminal chromium(III) ions. As pointed out before, the distortion of the central metal ion from a trigonal prismatic arrangement of the ligands toward an octahedron acts as a barrier toward the spin coupling between the terminal Cr(III) ions, as a result of the inefficient interaction between the orbitals of the oxime network and the Cr(III) ions. The terminal spins of $^3/_2$ are actually noninteracting in **11**, with the low-spin $d^6$ Fe(II) exhibiting the greatest twist angle of 34.8°. It is worth mentioning that EPR and magnetic measurements have recently unambiguously demonstrated the *intramolecular* nature of the physically significant exchange interactions operating between the terminal Cr(III) centers separated by a large distance of 7.14 Å in an analogous $Cr^{III}Zn^{II}Cr^{III}$ compound.[49]

**Acknowledgment.** This work was supported by the Fonds der Chemischen Industrie.

**Supporting Information Available:** Tables of crystal data and intensity measurements, interatomic bond distances and angles, positional and thermal parameters, and hydrogen atom coordinates (18 pages). Ordering information is given on any current masthead page.

IC971101+

(49) Burdinski, D.; Bill, E.; Birkelbach, F.; Lengen, M.; Trautwein, A. X.; Wieghardt, K.; Chaudhuri, P. To be submitted for publication.